

Reducing the Detrimental Effects of Saturation Phenomena in FRET Microscopy

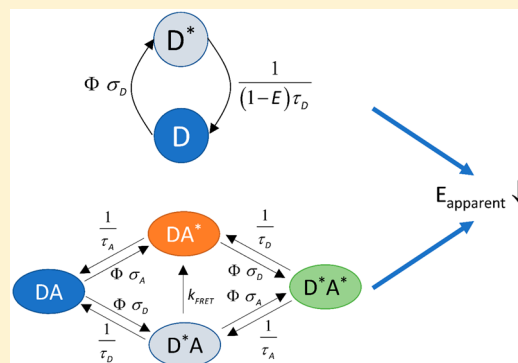
Tímea Szendi-Szatmári,[†] Ágnes Szabó,^{†,‡} János Szöllősi,^{†,‡} and Peter Nagy^{*,†,‡}

[†]Department of Biophysics and Cell Biology, Faculty of Medicine, University of Debrecen, Egyetem Square 1, 4032 Debrecen, Hungary

[‡]MTA-DE Cell Biology and Signaling Research Group, Faculty of Medicine, University of Debrecen, Debrecen, Hungary

S Supporting Information

ABSTRACT: Although Förster resonance energy transfer (FRET) is one of the most widely used biophysical methods in biology, the effect of high excitation intensity, leading to donor and acceptor saturation, has not been addressed previously. Here, we present a formalism for the experimental determination of the FRET efficiency at high excitation intensity when saturation of both the donor and the acceptor significantly affect conventional FRET calculations. We show that the proposed methodology significantly reduces the dependence of the FRET efficiency on excitation intensity, which otherwise significantly distorts FRET calculations at high excitation intensities commonly used in experiments. The work presented here adds additional rigor to the FRET-based investigation of protein interactions and strengthens the device independence of such results.



Investigation of protein interactions under physiological and pathological conditions can shed light on how cells function in health and disease. Förster resonance energy transfer (FRET) has become and still remains a key method for the analysis of protein interactions even in the era of super-resolution microscopy owing to its flexibility and relative ease of application.¹ In FRET, an excited donor transmits energy in a radiationless manner to a suitably oriented acceptor within a couple of nanometers if the absorption spectrum of the latter overlaps significantly with the emission spectrum of the former. This interaction typically leads to donor quenching, shortened donor lifetime, enhanced acceptor emission as well as changes in the anisotropy and photobleaching kinetics of the fluorophores.² Although all of these manifestations lend themselves to different measurement techniques, the most widespread application for measuring FRET is the intensity-based or ratiometric approach in which donor quenching, sensitized and directly excited acceptor fluorescence are measured.³ Although a lot of FRET efficiency-related parameters have been introduced,⁴ calculation of the energy transfer efficiency has the charm of being related to the studied interaction in a predictable way due to its solid physical background.⁵ Corrections for photobleaching and for the presence of noncomplexed donors and acceptors have been introduced in order to make the calculations more device-independent.^{6,7}

The first biological applications of FRET were suggested in the 1960s,⁸ followed by the development of intensity-based FRET approaches in fluorometry and flow cytometry.^{9,10} Due to the often weak fluorescence signal at physiological expression levels, the investigated targets are commonly

overexpressed, leading to mislocalization,¹¹ or stained with multiply labeled antibodies, resulting in diminished quantum yield and binding affinity.¹² Application of strong excitation intensity is also a possible way to increase the signal-to-noise ratio, but fluorophore saturation takes place at commonly applied excitation powers in confocal microscopy.¹³ If fluorophores are saturated, the emitted fluorescence is no longer linearly proportional to the excitation photon flux presenting a major obstacle to standardization. Despite this fact, its effect on intensity-based FRET calculations has not been evaluated. Therefore, the formalism developed for fluorometry and flow cytometry, in which fluorophore saturation is not an issue, has been applied without significant modifications to microscopy.¹⁴ Although FRET frustration, that is, the absence of FRET if acceptors are saturated, has already been considered,¹⁵ a complete formalism for intensity-based FRET considering saturation phenomena is not available. As opposed to photobleaching or detector saturation, which are easily identifiable problems related to high excitation intensities, fluorophore saturation is difficult to recognize, and if present, it can distort FRET calculations significantly.

Here, we show that the apparent FRET efficiency calculated according to conventional formulas significantly depends on the excitation photon flux. We present a formalism for evaluating FRET microscopy results taking saturation phenomena into account, and we demonstrate that this approach significantly reduces the dependence of the

Received: March 25, 2019

Accepted: April 17, 2019

Published: April 17, 2019

calculated FRET efficiency on excitation intensity. The proposed method is crucial for accurate and standardized FRET measurements at commonly applied excitation intensities in microscopy.

MATERIALS AND METHODS

Cell Line and Antibodies. The human breast-cancer cell line SKBR-3 overexpressing ErbB2 was obtained from the American Type Culture Collection (Rockville, MD) and cultured according to its specifications. For microscopic experiments, cells were grown in eight-well chambered coverglasses (Ibidi, Martinsried, Germany). ErbB2 was labeled by trastuzumab and pertuzumab. Trastuzumab and pertuzumab are humanized monoclonal antibodies against two nonoverlapping epitopes of ErbB2. Trastuzumab was purchased from Roche-Hungary (Budapest, Hungary) and pertuzumab was a kind gift from Genentech (South San Francisco, CA). AlexaFluor488, AlexaFluor546 and AlexaFluor647 dyes (Thermo Fisher Scientific, Waltham, MA) were conjugated to purified monoclonal antibodies according to the manufacturer's specifications.

Labeling of Cells with Antibodies. SKBR-3 cells were grown in 8-well chambered coverglass. Cells were washed twice with ice-cold phosphate-buffered saline (PBS, pH: 7.4). Cells were labeled with fluorescent antibodies at a concentration of 20 $\mu\text{g}/\text{mL}$ (~ 130 nM) in 150 μL of PBS containing 0.1% (w/v) BSA on ice in the dark for 30 min. For FRET measurements, cells were labeled with a mixture of donor-tagged and acceptor-tagged antibodies, while for the determination of parameter α and overspill coefficients, cells were labeled either with donor-conjugated or acceptor-tagged antibodies. In order to remove unbound antibodies the cells were washed twice with PBS followed by fixation in 1% formaldehyde.

Plasmids and Transfection. In order to measure FRET between fluorescent proteins, cells were transiently transfected with EGFP-mCherry coding for a fusion construct of the two fluorescent proteins separated by a linker (RDPPV).¹⁶ Spectral overspill factors were determined with cells transfected with pEGFP-C3 (Clontech Laboratories, Mountain View, CA) or with pmCherry-C3 (a kind gift of Julianna Volkó and György Vámosi, University of Debrecen). SKBR-3 cells grown on 8-well chambered coverglass were transfected with 0.5 μg plasmid/well using Lipofectamin2000 (Thermo Fisher) at a lipid/DNA ratio of 2:1 (v/w) according to the manufacturer's specification.

Confocal Microscopy. A Zeiss LSM 880 confocal laser scanning microscope (Carl Zeiss, Oberkochen, Germany) was used to image the samples. In order to measure FRET between AlexaFluor488-trastuzumab and AlexaFluor546-pertuzumab, excitation of the donor in the donor and FRET channels was performed at 488 nm, and emission was detected in the wavelength range of 500–530 and 550–610 nm, respectively. The acceptor was excited at 543 nm, and its emission was measured between 550 and 610 nm. During FRET measurements between AlexaFluor546-trastuzumab and AlexaFluor647-pertuzumab, AlexaFluor546-trastuzumab was excited by a 543 nm laser beam, and its emission was detected between 550 and 610 nm in the donor channel while FRET-sensitized fluorescence of the acceptor was measured between 635 and 755 nm. The excitation of AlexaFluor647-pertuzumab was performed at 633 nm, and its emission was detected between 635 and 755 nm. In order to determine FRET in

transfected cells the donor (EGFP) was excited at 488 nm and its emission was measured in the donor channel between 495 and 575 nm and FRET-sensitized emission of the acceptor was detected between 580–670 nm. The acceptor (mCherry) was excited by a 543 nm laser line and detected in the wavelength range of 575–695 nm. Fluorescence images were recorded as single optical sections using a 63 \times (NA = 1.4) oil immersion objective. A single field of view was measured at four different levels of increasing laser power (1–5–10–15%), followed by analyzing another field using decreasing excitation powers (15–10–5–1%). The measurements were carried out with a pinhole size of 1 Airy unit and a dwell time of 32.97 μs .

Measurement of Saturation of Mobile Fluorophores. Antibody stock solutions were diluted to 200 nM in PBS in order to measure their intensity. Since fluorophores in solution are mobile, photobleaching is negligible in this case. A relatively large volume (200 μL) of this antibody solution was added to a well of an 8-well chambered coverglass in order to prevent unpredictable reflections from the surface of a drop of a smaller volume of solution. Fluorescence intensity was measured as close to the coverglass as possible using excitation and emission settings described in the previous section in two different fields. The excitation intensity was gradually increased in one of the fields (1–5–10–15% laser power), while it was gradually decreased in the other field (15–10–5–1%). Since the two measurement types were identical within experimental error, demonstrated in Figure S8, the presented results are averages of both kinds of measurements. The measured fluorescence intensities were normalized to the intensity measured at the lowest excitation power followed by fitting eq S19 in the Supporting Information to these normalized values. The fitting provided the photon flux at the lowest excitation power.

Measurement of Laser Intensity. Laser power measurement was carried out with a Thorlabs (Newton, NJ) optical power meter (PM100D) equipped with a sensor for the spectral range of 350–1100 nm (S170C). The sensor was placed on the microscope stage after removing the objective. The laser power was measured using continuous illumination in spot scanning mode in order to prevent intermittent exposure of the sensor in raster scanning mode. The intensity of the lasers (488, 543, and 633 nm) was adjusted on a percent scale on the microscope, and the corresponding laser power was measured with the optical power meter, followed by converting it to photon flux considering the area of the focal spot and the energy of individual photons.¹⁷

Image Analysis. Image analysis was carried out in Matlab (MathWorks, Natick, MA) supplemented with the DipImage toolbox (Delft University of Technology, Delft, The Netherlands). Membrane pixels were identified with a custom-written implementation of the manually seeded watershed segmentation algorithm.¹⁸ The FRET efficiency and all the required correction parameters were calculated by rFRET in Matlab¹⁹ (<https://peternagy.webs.com/Matlab/rfret/rfret.zip>). The conventional formulas and those taking fluorophore saturation phenomena into account were also entered into an Excel sheet available at the following URL: https://peternagy.webs.com/Excel/FRET_at_saturation+photon_flux.xlsm.

RESULTS AND DISCUSSION

At high excitation photon flux FRET-induced quenching of donor fluorescence is mitigated due to the donor being almost instantaneously re-excited after relaxation due to energy

transfer (Figure 1). A quantitative consideration of this effect, shown in detail in the Supporting Information, predicts that

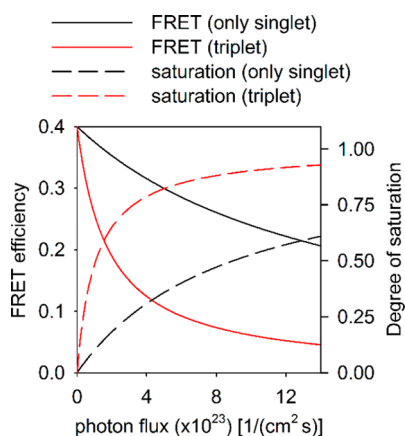


Figure 1. Donor saturation and its effect on the FRET efficiency. Fluorophore saturation in the absence and presence of the triplet state was calculated as a function of the excitation photon flux (dashed lines, $\tau = 4.1$ ns, $\epsilon = 41000$ M⁻¹ cm⁻¹, $k_{isc} = 7.3 \times 10^6$ s⁻¹, $k_{ph} = 10^6$ s⁻¹). The fluorescence lifetime and the molar absorption coefficient are those of AlexaFluor488, while the rate constants were chosen to correspond to a triplet lifetime of 1 μ s and a triplet quantum yield of 0.03. The fluorophore was assumed to serve as a donor in a FRET interaction characterized by an energy transfer efficiency of 0.4. This system was modeled both in the absence and presence of the triplet state, and the FRET efficiency was calculated from donor quenching using a conventional equation disregarding donor saturation (continuous lines).

the FRET efficiency evaluated from donor quenching (E_{apparent}) decreases as a function of fractional donor saturation (D_{sat}):

$$E_{\text{apparent}} = 1 - \frac{D_A^*}{D_{\text{noA}}^*} = \frac{(1 - D_{\text{sat}})E}{1 - D_{\text{sat}}E} \quad (1)$$

where E is the theoretical FRET efficiency, that is, the fraction of donors relaxing by FRET, D_A^* and D_{noA}^* are the concentration of excited donors in the presence and absence of acceptor, respectively. D_{sat} is the fractional saturation of the donor in the absence of FRET:

$$D_{\text{sat}} = \frac{\sigma_D \tau_D \Phi_D}{1 + \sigma_D \tau_D \Phi_D} \quad (2)$$

where σ_D and τ_D are the absorption cross-section and fluorescence lifetime of the donor, respectively, and Φ_D is the excitation photon flux. Rearrangement of eq 1 provides a way to correct the apparent FRET efficiency for donor saturation:

$$E = \frac{E_{\text{apparent}}}{1 + D_{\text{sat}}(E_{\text{apparent}} - 1)} \quad (3)$$

Since the excitation photon flux commonly used in confocal microscopy is within the range in which such saturation phenomena take place (Figure S1), we concluded that this issue merits further investigation. Equation 1 predicts that the excitation photon flux-dependent decline of E_{apparent} depends on the theoretical FRET efficiency with small energy transfer values affected to a higher extent (Figure S2). Since as much as 50–80% of the dye population accumulates in the triplet state

depending on fluorophore properties and the excitation power,¹³ intersystem crossing is expected to affect the apparent FRET efficiency as well. As shown in the Supporting Information, the apparent FRET efficiency derived from donor quenching declines as a function of fractional donor saturation, even if the triplet state is populated:

$$E_{\text{apparent}} = \frac{(1 - D_{\text{sat,T}})E}{1 - D_{\text{sat,T}}E} \quad (4)$$

where $D_{\text{sat,T}}$ is the fraction of donors in the excited singlet state normalized to the highest fraction of donors in the S_1 state in the presence of the triplet state:

$$D_{\text{sat,T}} = \frac{S_1}{\lim_{\Phi_D \rightarrow \infty} S_1} = \frac{D_{\text{sat}}(k_{isc} + k_{ph})}{D_{\text{sat}}k_{isc} + k_{ph}} \quad (5)$$

where k_{isc} is the rate constant of intersystem crossing from the S_1 to the T_1 state, and k_{ph} is the rate constant of phosphorescence, assumed to be equivalent to the pooled rate constant for relaxation of the T_1 state. Equation 4 has two important consequences: (i) it is not the fraction of donors in the excited state, but the normalized fractional saturation of the S_1 state, which determines the apparent decline of the FRET efficiency evaluated from donor quenching; and (ii) if the triplet state is populated, the apparent decrease of the FRET efficiency is even higher (Figure 1).

Since fluorescence is emitted from the S_1 state, the normalized fractional saturation of the S_1 state, given by eqs 2 and 5, can be simply determined by measuring the fractional saturation of fluorescence, enabling us to correct the apparent FRET efficiency for donor saturation. However, two problems must be solved before proceeding to the experimental determination of the FRET efficiency at fluorophore saturation. (i) The equation set taking frustrated FRET into consideration as well (see later) explicitly contains the photon flux; and (ii) k_{isc} and k_{ph} , required for accurate prediction of the normalized fractional saturation of fluorophores, are difficult to determine. Therefore, instead of measuring the photon flux with a laser power meter, a modified version of eq 2, shown in the Supporting Information, was fitted to the normalized fluorescence intensity of mobile fluorophores measured at different excitation photon fluxes (Figure S3). If the triplet state is populated, the photon flux determined from this fitting (Φ_{apparent}) will overestimate the real photon flux (eq S20 in the Supporting Information). If the triplet state of the dyes used is populated, but a model disregarding the triplet state (eq 3) is used to predict the apparent decrease of the FRET efficiency, substitution of this overestimated apparent photon flux into the model will lead to an accurate prediction of the apparent decrease of the FRET efficiency (eq S21 in the Supporting Information). Consequently, the proposed method only requires the determination of the apparent photon flux, easily available from fluorophore saturation, instead of the complicated measurement of the rate constants of transitions between the singlet and triplet states.

An equation set considering fluorophore saturation was derived in order to eliminate the photon flux-dependence of the calculated FRET efficiency in intensity-based FRET measurements. A parameter, designated by α , relating the detectability of excited acceptors to that of excited donors, is also required for intensity-based FRET measurements. Correction for the dependence of α on excitation photon

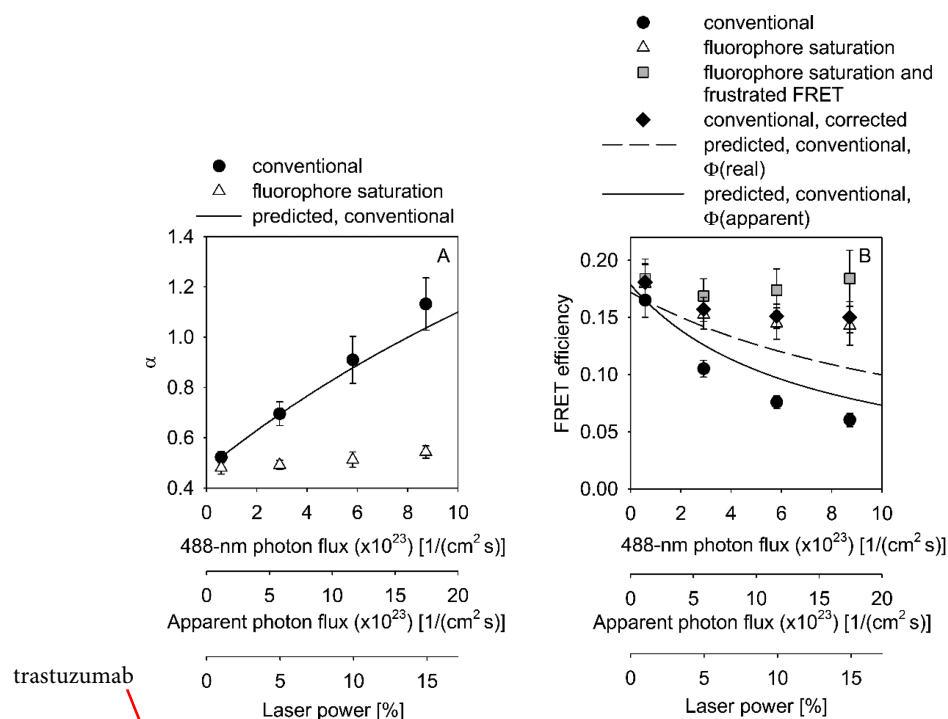


Figure 2. Evaluation of FRET in the AlexaFluor488–AlexaFluor546 donor–acceptor system. (A) SKBR-3 cells were labeled with AlexaFluor488-trastuzumab or AlexaFluor546-pertuzumab, and the fluorescence intensities of both the donor- and the acceptor-labeled samples were measured in the donor and FRET channels, respectively, at different intensities of the 488 nm laser. Parameter α was determined according to the conventional approach, disregarding fluorophore saturation (eq S23 in the Supporting Information) and using the proposed method considering saturation phenomena (eq S24 in the Supporting Information). The continuous line shows the predicted dependence of α , calculated in the conventional way, on excitation intensity (eq S26 in the Supporting Information). The real photon flux, the apparent photon flux (eq S20 in the Supporting Information) and the relative intensity on a percent scale, as adjusted on the microscope, are displayed on the horizontal axes in both parts of the figure. (B) Cells were labeled with both AlexaFluor488-trastuzumab and AlexaFluor546-pertuzumab and intensities were measured in the donor, FRET, and acceptor channels at different intensities of the 488 nm laser. FRET was evaluated in four different ways: conventional disregarding saturation phenomena (●), considering donor saturation (Δ), considering both donor saturation and FRET frustration (gray \square), and conventional calculation corrected for donor saturation according to eq 3 (\blacklozenge). The dashed and continuous lines show how the FRET efficiency calculated according to the conventional approach is expected to decline as a function of the real photon flux and the apparent photon flux, respectively, according to eq S7 in the Supporting Information. The photon flux of the acceptor-exciting, 543 nm laser was 9.5×10^{21} 1/(cm² s) corresponding to a laser power of 1%.

flux, determination of spectral correction factors, and details of the derivation are described in the Supporting Information. In the calculations discussed so far, frustrated FRET, that is, failure of FRET due to the acceptor being in the excited state, has not been considered. Another set of equations was derived that takes fluorophore saturation and frustrated FRET into consideration (see Supporting Information for details).

The aforementioned principles were used to evaluate FRET in the AlexaFluor488–AlexaFluor546 donor–acceptor pair. Both the FRET efficiency and α declined steeply as a function of the intensity of the donor-exciting laser in accordance with expectations (Figure 2). α corrected for fluorophore saturation was independent of the photon flux. The FRET efficiency was corrected in three different ways: (i) conventional calculation corrected according to eq 3; (ii) considering fluorophore saturation but disregarding frustrated FRET; and (iii) considering fluorophore saturation and frustrated FRET as well. The first two approaches, providing identical results, reduced the photon flux-dependence of the FRET efficiency, while the third one almost completely eliminated it. By comparing results obtained with changing only intensity of donor excitation, only that of acceptor excitation or both, we concluded that the donor excitation photon flux matters the most (Figure S4). These measurements were also carried out

with another donor–acceptor pair (AlexaFluor546–AlexaFluor647) leading to identical results (Figure S5).

The approach was also applied to a donor–acceptor pair consisting of two fluorescent proteins (GFP+mCherry). The equation sets were slightly modified in order to determine both the FRET efficiency and α from the same measurement²⁰ (see Supporting Information for details). These measurements also confirmed that the equation sets considering saturation phenomena successfully eliminate the dependence of the FRET efficiency on the excitation photon flux (Figure S6). The estimated and real photon fluxes for GFP were identical in accordance with its very low triplet conversion probability.²¹

Elimination of the strong dependence of the calculated FRET efficiency on excitation photon flux argues for the validity of the underlying assumptions of the proposed method, even though simplifications were introduced for the sake of applicability. From among the multitude of de-excitation pathways available for excited fluorophores, photobleaching and singlet–singlet annihilation, both of which were shown to influence FRET calculations,^{6,22} were neglected. Singlet–singlet annihilation is unlikely to occur significantly in the experimental systems presented in the manuscript for the following reasons: (i) It was shown to eliminate the excitation power-dependence of the apparent FRET efficiency.²² The

mere existence of the excitation photon flux dependence of the calculated FRET efficiency implies that singlet–singlet annihilation does not take place in our systems. (ii) In a complex of one donor and one acceptor singlet–singlet annihilation occurs when both fluorophores are in the excited state (D^*A^*). The fraction of such complexes from among all donor–acceptor pairs containing excited donors ($D^*A + D^*A^*$) was determined according to eq S32. These calculations allowed us to conclude that the population density of D^*A^* is high only at large FRET values (Figure S7). Since FRET values above 0.3–0.4 are rarely obtained in cellular FRET measurements, neglecting singlet–singlet annihilation is a reasonable simplifying assumption in such experiments. Photobleaching can also influence FRET measurements by decreasing the amount and density of acceptors and donors and by modifying the donor/acceptor ratio.⁶ Depending on whether the donor and acceptor are randomly distributed or clustered and also on the size of clusters, photobleaching-induced changes in the FRET efficiency range between considerable and negligible.^{23–26} Although dyes underwent photobleaching, resulting in intensity decreases up to ~30% in the three experimental systems investigated in the manuscript, photobleaching did not have a significant effect on the calculated FRET efficiencies, since the FRET values were insensitive to the duration of previous exposure to excitation light (Figure S8). If FRET values calculated in the conventional way or by any of the methods proposed in the current manuscript turn out to be sensitive to bleaching, they should be corrected for bleaching after careful consideration of the applicability of the correction formula.

CONCLUSION

In conclusion, we derived and applied a formalism for the evaluation of microscopic FRET experiments at photon fluxes leading to fluorophore saturation and frustrated FRET. The proposed method, incorporated into the rFRET Matlab program,¹⁹ significantly reduces the dependence of the energy transfer efficiency on excitation intensity, which would otherwise distort the measurement. Saturation phenomena must not be overlooked in microscopic FRET measurements in order to add rigor to and increase the device-independence of such experiments.

ASSOCIATED CONTENT

Supporting Information

The Supporting Information is available free of charge on the ACS Publications website at DOI: 10.1021/acs.analchem.9b01504.

Eight figures, Matlab code of functions for evaluating FRET experiments and detailed derivation of the theory of intensity-based FRET calculations in the presence of fluorophore saturation (PDF)

AUTHOR INFORMATION

Corresponding Author

*E-mail: nagyp@med.unideb.hu.

ORCID

Peter Nagy: 0000-0002-7466-805X

Notes

The authors declare no competing financial interest.

ACKNOWLEDGMENTS

The work was supported by research grants from the National Research, Development and Innovation Office, Hungary (K120302, GINOP-2.3.2-15-2016-00020, GINOP-2.3.2-15-2016-00044).

REFERENCES

- (1) Grecco, H. E.; Verveer, P. J. *ChemPhysChem* **2011**, *12*, 484–490.
- (2) Clegg, R. M. In *Laboratory Techniques in Biochemistry and Molecular Biology*, Gadella, T. W. J., Ed.; Elsevier, 2009; pp 1–57.
- (3) Jares-Erijman, E. A.; Jovin, T. M. *Nat. Biotechnol.* **2003**, *21*, 1387–1395.
- (4) Berney, C.; Danuser, G. *Biophys. J.* **2003**, *84*, 3992–4010.
- (5) Zeug, A.; Woehler, A.; Neher, E.; Ponimaskin, E. G. *Biophys. J.* **2012**, *103*, 1821–1827.
- (6) Zal, T.; Gascoigne, N. R. *Biophys. J.* **2004**, *86*, 3923–3939.
- (7) Wlodarczyk, J.; Woehler, A.; Kobe, F.; Ponimaskin, E.; Zeug, A.; Neher, E. *Biophys. J.* **2008**, *94*, 986–1000.
- (8) Stryer, L.; Haugland, R. P. *Proc. Natl. Acad. Sci. U. S. A.* **1967**, *58*, 719–726.
- (9) Szöllősi, J.; Trón, L.; Damjanovich, S.; Helliwell, S. H.; Arndt-Jovin, D.; Jovin, T. M. *Cytometry* **1984**, *5*, 210–216.
- (10) Trón, L.; Szöllősi, J.; Damjanovich, S.; Helliwell, S. H.; Arndt-Jovin, D. J.; Jovin, T. M. *Biophys. J.* **1984**, *45*, 939–946.
- (11) Snapp, E. *Curr. Protocols Cell Biol.* **2005**, *27*, 21.4.1–21.4.13.
- (12) Szabó, A.; Szendi-Szalmáry, T.; Ujlaky-Nagy, L.; Rádi, I.; Vereb, G.; Szöllősi, J.; Nagy, P. *Biophys. J.* **2018**, *114*, 688–700.
- (13) Tsiernis, R. Y.; Ernst, L.; Waggoner, A. In *Handbook of Biological Confocal Microscopy*; Pawley, J. B., Ed.; Springer: New York, 2006; pp 338–352.
- (14) Nagy, P.; Vámosi, G.; Bodnár, A.; Lockett, S. J.; Szöllősi, J. *Eur. Biophys. J.* **1998**, *27*, 377–389.
- (15) Beutler, M.; Makrogianneli, K.; Vermeij, R. J.; Keppler, M.; Ng, T.; Jovin, T. M.; Heintzmann, R. *Eur. Biophys. J.* **2008**, *38*, 69–82.
- (16) Renz, M.; Daniels, B. R.; Vámosi, G.; Arias, I. M.; Lippincott-Schwartz, J. *Proc. Natl. Acad. Sci. U. S. A.* **2012**, *109*, E2989–2997.
- (17) Wilhelm, S. *Confocal Laser Scanning Microscopy*; Carl Zeiss: Jena.
- (18) Gonzalez, R. C.; Woods, R. E.; Eddins, S. L. In *Digital Image Processing Using Matlab*, Gonzalez, R. C., Woods, R. E., Eddins, S. L., Eds.; Pearson Prentice Hall: Upper Saddle River, NJ, 2004; pp 417–425.
- (19) Nagy, P.; Szabó, A.; Váradi, T.; Kovács, T.; Batta, G.; Szöllősi, J. *Cytometry, Part A* **2016**, *89*, 376–384.
- (20) Szalóki, N.; Doan-Xuan, Q. M.; Szöllősi, J.; Tóth, K.; Vámosi, G.; Bacsó, Z. *Cytometry, Part A* **2013**, *83*, 818–829.
- (21) Widengren, J.; Rigler, R. *Cell Mol. Biol. (Noisy-le-grand)* **1998**, *44*, 857–879.
- (22) Nettels, D.; Haenni, D.; Maillot, S.; Gueye, M.; Barth, A.; Hirschfeld, V.; Hubner, C. G.; Leonard, J.; Schuler, B. *Phys. Chem. Chem. Phys.* **2015**, *17*, 32304–32315.
- (23) Kenworthy, A. K.; Edidin, M. *J. Cell Biol.* **1998**, *142*, 69–84.
- (24) Kenworthy, A. K.; Petranova, N.; Edidin, M. *Mol. Biol. Cell* **2000**, *11*, 1645–1655.
- (25) Hur, K. H.; Macdonald, P. J.; Berk, S.; Angert, C. I.; Chen, Y.; Mueller, J. D. *PLoS One* **2014**, *9*, No. e97440.
- (26) Yeow, E. K.; Clayton, A. H. *Biophys. J.* **2007**, *92*, 3098–3104.

Correction to Reducing the Detrimental Effects of Saturation Phenomena in FRET Microscopy

Tímea Szendi-Szatmári, Ágnes Szabó, János Szöllősi, and Peter Nagy*

Anal. Chem. **2019**, *91*, 6378–6382. DOI: [10.1021/acs.analchem.9b01504](https://doi.org/10.1021/acs.analchem.9b01504)



Cite This: <https://dx.doi.org/10.1021/acs.analchem.0c01481>



Read Online

ACCESS |



Metrics & More



Article Recommendations



Supporting Information

We would like to correct the caption to [Figure 2](#) in our original paper. The names of the antibodies pertaining to part A of the figure were incorrectly displayed in the figure caption.

The Supporting Information file published with the original paper also had an error in the names of the antibodies. The corrected [Supporting Information](#) file is published with this Addition and Correction.

■ ASSOCIATED CONTENT

SI Supporting Information

The Supporting Information is available free of charge at <https://pubs.acs.org/doi/10.1021/acs.analchem.0c01481>.

Eight figures, Matlab code of functions for evaluating FRET experiments and detailed derivation of the theory of intensity-based FRET calculations in the presence of fluorophore saturation ([PDF](#))

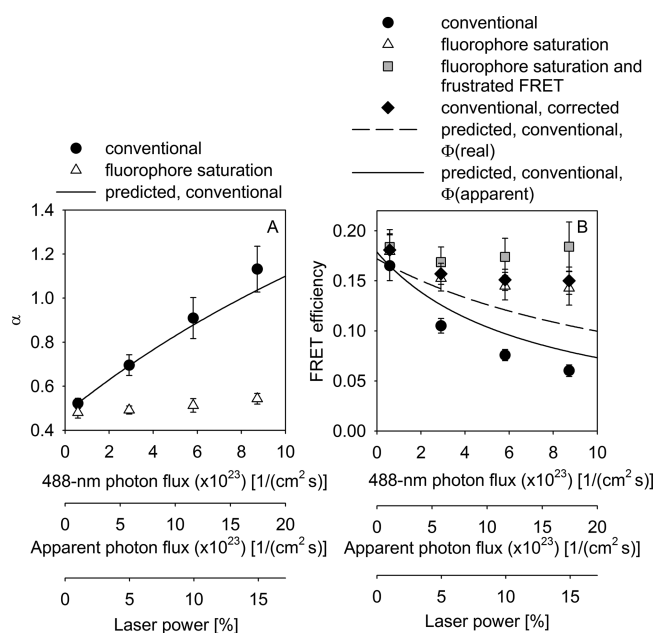


Figure 2. Evaluation of FRET in the AlexaFluor488–AlexaFluor546 donor–acceptor system. (A) SKBR-3 cells were labeled with AlexaFluor488-trastuzumab or AlexaFluor546-trastuzumab, and the fluorescence intensities of both the donor- and the acceptor-labeled samples were measured in the donor and FRET channels, respectively, at different intensities of the 488 nm laser. Parameter α was determined according to the conventional approach disregarding fluorophore saturation (equation S23 in the Supporting Information) and using the proposed method considering saturation phenomena (equation S24 in the Supporting Information). The continuous line shows the predicted dependence of α , calculated in the conventional way, on excitation intensity (equation S26 in the Supporting Information). The real photon flux, the apparent photon flux (equation S20 in the Supporting Information), and the relative intensity on a percent scale, as adjusted on the microscope, are displayed on the horizontal axes in both parts of the figure. (B) Cells were labeled with both AlexaFluor488-trastuzumab and AlexaFluor546-pertuzumab and intensities were measured in the donor, FRET, and acceptor channels at different intensities of the 488 nm laser. FRET was evaluated in four different ways: conventional disregarding saturation phenomena (\bullet), considering donor saturation (\triangle), considering both donor saturation and FRET frustration (gray \square), and conventional calculation corrected for donor saturation according to eq 3 (\blacklozenge). The dashed and continuous lines show how the FRET efficiency calculated according to the conventional approach is expected to decline as a function of the real photon flux and the apparent photon flux, respectively, according to eq 1. The photon flux of the acceptor-exciting, 543 nm laser was $9.5 \times 10^{21} \text{ 1}/(\text{cm}^2 \text{ s})$ corresponding to a laser power of 1%.

Supplementary Information

Reducing the detrimental effects of saturation phenomena in FRET microscopy

Tímea Szendi-Szatmári, Ágnes Szabó, János Szöllősi, Peter Nagy*

*To whom correspondence should be addressed (nagyp@med.unideb.hu)

SUPPLEMENTARY RESULTS

Effect of donor saturation on the apparent FRET efficiency

Let us first investigate the extent of fluorophore saturation in the absence of FRET. For the moment it is assumed that the fluorophore has only ground and excited singlet states. In equilibrium the number of ground state donors getting excited is equal to the number of excited donors relaxing. This condition is summarized by the following matrix equation:

$$\begin{pmatrix} 0 \\ 0 \\ D_{all} \end{pmatrix} = \begin{pmatrix} -\Phi_D \sigma_D & \frac{1}{\tau_D} \\ \Phi_D \sigma_D & -\frac{1}{\tau_D} \\ 1 & 1 \end{pmatrix} \begin{pmatrix} D \\ D^* \end{pmatrix} \quad (S1)$$

where Φ_D is the photon flux of the donor-exciting laser, σ_D and τ_D are the absorption cross-section and fluorescence lifetime, respectively, of the donor. D and D^* are the concentration of donors in the ground and excited states, respectively, and D_{all} is the total concentration of donors. The solutions for D and D^* are shown below:

$$D = \frac{D_{all}}{1 + \sigma_D \tau_D \Phi_D}, \quad D^* = \frac{D_{all} \sigma_D \tau_D \Phi_D}{1 + \sigma_D \tau_D \Phi_D} \quad (S2)$$

By designating fractional fluorophore saturation by D_{sat} , the excited fluorophore population can be described by the following equation:

$$D_{sat} = \frac{\sigma_D \tau_D \Phi_D}{1 + \sigma_D \tau_D \Phi_D} \Rightarrow D^* = D_{all} D_{sat} \quad (S3)$$

The most obvious and direct manifestation of FRET is donor quenching, i.e. its decreased fluorescence intensity in the presence of an acceptor. Let us investigate the extent of donor quenching if fluorophore saturation cannot be neglected. By applying the principle used for a lone donor, the steady-state is described by the following matrix equation:

$$\begin{pmatrix} 0 \\ 0 \\ 0 \\ 0 \\ D_{all} \\ A_{all} \end{pmatrix} = \begin{pmatrix} -\Phi_D \sigma_D & \frac{1}{(1-E)\tau_D} & 0 & 0 \\ \Phi_D \sigma_D & -\frac{1}{(1-E)\tau_D} & 0 & 0 \\ 0 & -\frac{E}{(1-E)\tau_D} & -\Phi_D \sigma_A & \frac{1}{\tau_A} \\ 0 & \frac{E}{(1-E)\tau_D} & \Phi_D \sigma_A & -\frac{1}{\tau_A} \\ 1 & 1 & 0 & 0 \\ 0 & 0 & 1 & 1 \end{pmatrix} \begin{pmatrix} D \\ D^* \\ A \\ A^* \end{pmatrix} \quad (S4)$$

where E is the FRET efficiency, σ_A and τ_A are the absorption cross-section of the acceptor and its fluorescence lifetime, respectively. A and A^* are the concentrations of acceptors in the ground and excited states, respectively, and A_{all} is the total concentration of acceptors. The solutions for D^* and A^* are shown below:

$$D^* = \frac{D_{all} (1-E) \sigma_D \tau_D \Phi_D}{1 + (1-E) \sigma_D \tau_D \Phi_D} \quad (S5)$$

$$A^* = \frac{\tau_A \Phi_D \left(A_{all} \sigma_A + \frac{D_{all} E \sigma_D}{1 + (1-E) \sigma_D \tau_D \Phi_D} \right)}{1 + \sigma_A \tau_A \Phi_D}$$

These expressions can be simplified using the fractional saturation of fluorophores defined previously by equation (S3):

$$D^* = \frac{D_{all} D_{sat} (1-E)}{1 - D_{sat} E} \quad (S6)$$

$$A^* = A_{All} A_{sat} + \frac{(1 - A_{sat}) D_{all} D_{sat} E \tau_A}{(1 - D_{sat} E) \tau_D}$$

Since the fluorescence intensity of the donor is proportional to the concentration of donors in the excited state, the apparent FRET efficiency calculated from donor quenching can now be determined as follows:

$$E_{apparent} = 1 - \frac{D_A^*}{D_{no A}^*} = \frac{E}{1 + (1-E) \sigma_D \tau_D \Phi_D} = \frac{(1 - D_{sat}) E}{1 - D_{sat} E} \quad (S7)$$

where D_A^* and $D_{no A}^*$ are the concentrations of excited donors in the presence and absence of the acceptor, respectively, and E is the theoretical FRET efficiency that can be observed when the photon flux approaches zero (donor saturation is negligible). This equation predicts that $E_{apparent}$ declines as a function of donor saturation in a manner also influenced by the theoretical FRET efficiency (Fig. S2). Equation (S7) provides an obvious way for correcting the calculated, apparent FRET efficiency for donor saturation:

$$E = \frac{E_{apparent}}{1 + D_{sat} (E_{apparent} - 1)} \quad (S8)$$

Effect of the triplet state on donor saturation-dependent change in apparent FRET efficiency

Most fluorophores undergo intersystem crossing to the triplet state significantly influencing fluorophore saturation. The following matrix equation describes the equilibrium population densities of the S_0 , S_1 and T_1 states of the donor in the absence of FRET:

$$\begin{pmatrix} 0 \\ 0 \\ 0 \\ D_{all} \end{pmatrix} = \begin{pmatrix} -\Phi_D \sigma_D & \frac{1}{\tau_D} - k_{isc} & k_{ph} \\ \Phi_D \sigma_D & -\frac{1}{\tau_D} & 0 \\ 0 & k_{isc} & -k_{ph} \\ 1 & 1 & 1 \end{pmatrix} \begin{pmatrix} S_0 \\ S_1 \\ T_1 \end{pmatrix} \quad (S9)$$

where k_{isc} is the rate constant of intersystem crossing. Without loss of generality it was assumed that fluorophores in the T_1 state relax to the S_0 state only by phosphorescence. Therefore, k_{ph} is the overall rate constant of triplet state relaxation. The solution of the above equation for the equilibrium densities is as follows:

$$\begin{aligned} S_0 &= \frac{D_{all} k_{ph}}{k_{ph} + (k_{isc} + k_{ph}) \sigma_D \tau_D \Phi_D} \\ S_1 &= \frac{D_{all} k_{ph} \sigma_D \tau_D \Phi_D}{k_{ph} + (k_{isc} + k_{ph}) \sigma_D \tau_D \Phi_D} \\ T_1 &= \frac{D_{all} k_{isc} \sigma_D \tau_D \Phi_D}{k_{ph} + (k_{isc} + k_{ph}) \sigma_D \tau_D \Phi_D} \end{aligned} \quad (S10)$$

The maximum fluorescence intensity emitted by the donor at an infinitely large photon flux is given by the following equation:

$$\lim_{\Phi_D \rightarrow \infty} \left(\frac{D_{all} k_{ph} \sigma_D \tau_D \Phi_D}{k_{ph} + (k_{isc} + k_{ph}) \sigma_D \tau_D \Phi_D} \right) = \frac{k_{ph} D_{all}}{k_{isc} + k_{ph}} \quad (S11)$$

Similar to equation (S3) fractional saturation of the donor in the presence of the triplet state can be given as follows:

$$D_{sat,T} = \frac{\frac{D_{all} k_{ph} \sigma_D \tau_D \Phi_D}{k_{ph} + (k_{isc} + k_{ph}) \sigma_D \tau_D \Phi_D}}{\frac{k_{ph} D_{all}}{k_{isc} + k_{ph}}} = \frac{(k_{isc} + k_{ph}) \sigma_D \tau_D \Phi_D}{k_{ph} + (k_{isc} + k_{ph}) \sigma_D \tau_D \Phi_D} \quad (S12)$$

The previous equation can be simplified even further using the expression for D_{sat} :

$$D_{sat,T} = \frac{D_{sat} (k_{isc} + k_{ph})}{D_{sat} k_{isc} + k_{ph}} \quad (S13)$$

Let us now express the equilibrium population densities of the S_0 , S_1 and T_1 states of the donor in the presence of FRET:

$$\begin{pmatrix} 0 \\ 0 \\ 0 \\ D_{all} \end{pmatrix} = \begin{pmatrix} -\Phi_D \sigma_D & \frac{1+(E-1)k_{isc}\tau_D}{(1-E)\tau_D} & k_{ph} \\ \Phi_D \sigma_D & -\frac{1}{(1-E)\tau_D} & 0 \\ 0 & k_{isc} & -k_{ph} \\ 1 & 1 & 1 \end{pmatrix} \begin{pmatrix} S_0 \\ S_1 \\ T_1 \end{pmatrix} \quad (S14)$$

The time constant for the $S_1 \rightarrow S_0$ transition was determined according to the following consideration:

$$\left. \begin{aligned} \tau_{DA} &= \frac{1}{k_f + k_{nf} + k_{isc} + k_{fret}} \\ \tau_D &= \frac{1}{k_f + k_{nf} + k_{isc}} \\ E &= 1 - \frac{\tau_{DA}}{\tau_D} \\ \tau_{S1 \rightarrow S0} &= \frac{1}{k_f + k_{nf} + k_{fret}} \end{aligned} \right\} \tau_{S1 \rightarrow S0} = \frac{\tau_D (1-E)}{1 + (E-1)k_{isc}\tau_D} \quad (S15)$$

Solution of equation (S14) for S_0 , S_1 and T_1 is given below:

$$\begin{aligned}
 S_0 &= \frac{k_{ph} D_{all}}{(E-1)(k_{isc} + k_{ph})\sigma_D \tau_D \Phi_D - k_{ph}} \\
 S_1 &= \frac{(E-1)k_{ph} D_{all} \sigma_D \tau_D \Phi_D}{(E-1)(k_{isc} + k_{ph})\sigma_D \tau_D \Phi_D - k_{ph}} \\
 T_1 &= \frac{(E-1)k_{isc} D_{all} \sigma_D \tau_D \Phi_D}{(E-1)(k_{isc} + k_{ph})\sigma_D \tau_D \Phi_D - k_{ph}}
 \end{aligned} \tag{S16}$$

Let us express the apparent FRET efficiency, similarly to equation (S7), in the presence of the triplet state:

$$E_{apparent} = 1 - \frac{S_{1,A}}{S_{1,no A}} = \frac{E k_{ph}}{(E-1)(k_{isc} + k_{ph})\sigma_D \tau_D \Phi_D - k_{ph}} \tag{S17}$$

where $S_{1,A}$ and $S_{1, no A}$ are the equilibrium concentrations of the S_1 state in the presence of the acceptor (equation (S16)) and its absence (equation (S10)), respectively. By using the fractional donor saturation defined by equation (S12) the previous expression can be significantly simplified:

$$E_{apparent} = \frac{(1 - D_{sat,T})E}{1 - D_{sat,T}} \tag{S18}$$

Although the triplet state significantly modifies the degree of saturation of the S_1 state, comparison of equation (S7) and (S18) shows that the apparent FRET efficiency only depends on the degree of saturation of the S_1 state independent of whether the triplet state is populated.

Determination of fluorophore saturation and the apparent photon flux

Since photobleaching is negligible if mobile fluorophores are investigated, the degree of fluorophore saturation can be determined by measuring the fluorescence intensity of mobile fluorophores as a function of excitation photon flux. Since photon flux was found to be strictly linear to the percental laser intensity adjusted on the microscope (see Fig. S1), the fluorescence intensity, normalized to the intensity (I_1) measured at the lowest excitation power, can be calculated according to the following equation:

$$\left. \begin{aligned} I_1 &\sim \frac{\sigma \tau \Phi_1}{1 + \sigma \tau \Phi_1} \\ I_k &\sim \frac{\sigma \tau k \Phi_1}{1 + \sigma \tau k \Phi_1} \end{aligned} \right\} I_{k, norm} = 1 + \frac{k-1}{1 + k \sigma \tau \Phi_1} \quad (S19)$$

where k shows how many times the laser power was higher when measuring I_k compared to the lowest excitation intensity, Φ_1 , used for I_1 . By fitting equation (S19) to the normalized, measured intensities Φ_1 can be determined. Although the photon flux can be relatively easily calculated by measuring laser power at the sample and considering the energy of individual photons and the area of the point spread function, we resorted to determining it from fitting for the following reasons: (i) the point spread function of the objective in the sample is usually unknown; (ii) we wanted to correct for the effect of the triplet state on the fractional saturation of S_1 as explained below.

The photon flux is a variable in the equations to be presented in the next sections for the experimental determination of the FRET efficiency from intensity-based measurements. The model used for deriving these equations does not include the triplet state since rate constants for the $S_1 \rightarrow T_1$ and $T_1 \rightarrow S_0$ transitions are typically unknown, and our aim was to establish a method, which can be used without the need to determine these constants from photophysical measurements. Equation (S19) for determining the photon flux also disregards the triplet state. Since this equation provides an estimate for the photon flux according to the fractional saturation of fluorescence, which is influenced by the triplet state, the photon flux will be misestimated. The magnitude of this error can be calculated by considering that a model disregarding the triplet state (described by equation (S3)) is used for describing a fluorophore whose triplet state is populated (described by equation (S12)):

$$\frac{(k_{isc} + k_{ph}) \sigma \tau \Phi_{real}}{k_{ph} + (k_{isc} + k_{ph}) \sigma \tau \Phi_{real}} = \frac{\sigma \tau \Phi_{apparent}}{1 + \sigma \tau \Phi_{apparent}} \Rightarrow \Phi_{apparent} = \frac{k_{isc} + k_{ph}}{k_{ph}} \Phi_{real} \quad (S20)$$

where Φ_{real} is the real photon flux and $\Phi_{apparent}$ is the one estimated from the model disregarding the triplet state. Let us substitute this misestimated photon flux into the equation for calculating the apparent FRET efficiency in a model neglecting the triplet state (equation (S7)):

$$\left. \begin{aligned} E_{\text{apparent}} &= \frac{E}{1 + (1-E)\sigma_D \tau_D \Phi_{\text{apparent}}} \\ \Phi_{\text{apparent}} &= \frac{k_{\text{isc}} + k_{\text{ph}}}{k_{\text{ph}}} \Phi_{\text{real}} \end{aligned} \right\} E_{\text{apparent}} = \frac{E k_{\text{ph}}}{(E-1)(k_{\text{isc}} + k_{\text{ph}})\sigma_D \tau_D \Phi_{\text{real}} - k_{\text{ph}}} \quad (\text{S21})$$

This equation provides a solution for the apparent FRET efficiency identical to the one in which the triplet state was involved (equation (S17)) showing that the photon flux misestimated due to neglecting the triplet state leads to a correct FRET efficiency for a system involving the triplet state when this misestimated photon flux is substituted into the model disregarding the triplet state. For this reason, this estimated, apparent photon flux will be used in the equations providing a solution for the FRET efficiency from intensity-based measurements in the next sections.

Overspill factors and parameter α considering saturation phenomena

Before one can solve the intensity-based equations, the effect of fluorophore saturation on overspill factors and parameter α must be determined. α expresses the ratio of the detection efficiency of an excited donor in the donor channel to the detection efficiency of an excited acceptor in the FRET channel:

$$\alpha = \frac{Q_A \eta_{A,2}}{Q_D \eta_{D,1}} \quad (\text{S22})$$

where Q_D and Q_A are the fluorescence quantum yields of the donor and the acceptor, respectively, while $\eta_{D,1}$ and $\eta_{A,2}$ are the detection efficiencies of donor photons in the first (donor) channel and that of acceptor photons in the second (FRET) channel, respectively. According to one of the experimental methods for determining α ¹, a sample is labeled with a donor-conjugated antibody against a certain epitope. The fluorescence intensity of this sample is designated by M_D . The same kind of cells are labeled with the acceptor-conjugated version of the same antibody. The intensity of this latter sample is designated by M_A . From equations describing M_D and M_A parameter α can be determined:

$$\left. \begin{aligned} M_D &\sim L_D \sigma_{D(D)} \Phi_D Q_D \eta_{D,1} \\ M_A &\sim L_A \sigma_{A(D)} \Phi_D Q_A \eta_{A,2} \end{aligned} \right\} \alpha = \frac{M_A L_D \sigma_{D(D)}}{M_D L_A \sigma_{A(D)}} \quad (\text{S23})$$

where L_D and L_A are the degrees of labeling of the donor-tagged and acceptor-tagged antibodies, respectively, $\sigma_{D(D)}$ is the absorption cross-section of the donor at the excitation wavelength of the donor and $\sigma_{A(D)}$ is the absorption cross-section of the acceptor at the excitation wavelength of the donor. However, equation (S23) does not take fluorophore saturation into consideration. If this phenomenon is also considered, α takes the following form:

$$\left. \begin{array}{l} M_D \sim L_D D_{sat,D} k_{f,D} \eta_{D,1} \\ M_A \sim L_A A_{sat,D} k_{f,A} \eta_{A,2} \end{array} \right\} \alpha_{sat} = \frac{M_A L_D D_{sat,D} \tau_A}{M_D L_A A_{sat,D} \tau_D} \quad (S24)$$

where $D_{sat,D}$ and $A_{sat,D}$ are the fractional saturations of the donor and the acceptor, respectively, at the donor excitation wavelength, τ_D and τ_A are the fluorescence lifetimes of the donor and the acceptor, respectively, and $k_{f,D}$ and $k_{f,A}$ are the fluorescence rate constants of the donor and the acceptor, respectively. In order to show the validity of the assumptions behind equation (S24) the limit of α_{sat} was calculated at infinitesimally low laser intensity:

$$\lim_{\Phi_D \rightarrow 0} \frac{M_A L_D D_{sat,D} \tau_A}{M_D L_A A_{sat,D} \tau_D} = \lim_{\Phi_D \rightarrow 0} \frac{M_A L_D \frac{\sigma_{D(D)} \tau_D \Phi_D}{1 + \sigma_{D(D)} \tau_D \Phi_D} \tau_A}{M_D L_A \frac{\sigma_{A(D)} \tau_A \Phi_D}{1 + \sigma_{A(D)} \tau_A \Phi_D} \tau_D} = \frac{M_A L_D \sigma_{D(D)}}{M_D L_A \sigma_{A(D)}} \quad (S25)$$

Since the limit of α_{sat} at $\Phi \rightarrow 0$ is equal to α derived previously and also in the original publication¹, assumptions incorporated into equation (S24) are justified. Considering fluorophore saturation it can be predicted how α , determined according to the conventional formula, is distorted as a function of fluorophore saturation:

$$\alpha_{apparent} = \alpha \frac{A_{sat,D} \sigma_{D(D)} \tau_D}{D_{sat,D} \sigma_{A(D)} \tau_A} \quad (S26)$$

Overspill factors present in the equations describing intensity-based FRET measurements are summarized in Supplementary Table 1.

Parameter	Sym- bol	Experimental value		Theoretical equation	
		without saturation	with saturation	without saturation	with saturation
Donor overspill to FRET channel	S_1		$\frac{I_{D,2}}{I_{D,1}}$		$\frac{\eta_{D,2}}{\eta_{D,1}}$
Donor overspill to acceptor channel	S_3		$\frac{I_{D,3}}{I_{D,1}}$	$\frac{\Phi_A \sigma_{D(A)} \eta_{D,3}}{\Phi_D \sigma_{D(D)} \eta_{D,1}}$	$\frac{D_{sat,A} \eta_{D,3}}{D_{sat,D} \eta_{D,1}}$
Acceptor overspill to FRET channel	S_2		$\frac{I_{A,2}}{I_{A,3}}$	$\frac{\Phi_D \sigma_{A(D)} \eta_{A,2}}{\Phi_A \sigma_{A(A)} \eta_{A,3}}$	$\frac{A_{sat,D} \eta_{A,2}}{A_{sat,A} \eta_{A,3}}$
Acceptor overspill to donor channel	S_4		$\frac{I_{A,1}}{I_{A,3}}$	$\frac{\Phi_D \sigma_{A(D)} \eta_{A,1}}{\Phi_A \sigma_{A(A)} \eta_{A,3}}$	$\frac{A_{sat,D} \eta_{A,1}}{A_{sat,A} \eta_{A,3}}$

Supplementary Table 1. Overspill factors for the intensity-based determination of the FRET efficiency. $I_{D,1}$, $I_{D,2}$, $I_{D,3}$ are the intensities of the donor-only sample in the donor, FRET and acceptor channels, respectively. $I_{A,1}$, $I_{A,2}$, $I_{A,3}$ are the intensities of the acceptor-only sample in the donor, FRET and acceptor channels, respectively. Φ_D and Φ_A stand for the photon flux of the donor-exciting and acceptor-exciting lasers, respectively. $\eta_{D,x}$ and $\eta_{A,x}$ designate the detection efficiency of donor and acceptor photons, respectively, in the x^{th} fluorescence channel. $D_{sat,D}$ and $D_{sat,A}$ are the degree of saturation of the donor at the donor and acceptor excitation wavelength, respectively, and $A_{sat,D}$ and $A_{sat,A}$ are the same parameters for the acceptor. $\sigma_{D(D)}$ and $\sigma_{D(A)}$ are the absorption cross-sections of the donor at the excitation wavelength of the donor and acceptor, respectively, and $\sigma_{A(D)}$ and $\sigma_{A(A)}$ are the same parameters for the acceptor.

Determination of the FRET efficiency considering donor saturation in an intensity-based experiment

In an intensity-based FRET measurement three intensities, designated by I_1 - I_3 , are measured. In the donor channel, I_1 , fluorophores are excited at the donor excitation wavelength and fluorescence is recorded in the donor emission range. Fluorescence in the acceptor channel, I_3 , is excited at the acceptor excitation wavelength, and emission is recorded in the acceptor emission range. In the FRET channel, I_2 , the donor excitation wavelength is combined with detection in the acceptor emission range. Using the solutions for D^* and A^* (equation (S6)), the overspill coefficients and parameter α from Supplementary Table 1 the I_1 - I_3 intensities were written to form the following set of equations:

$$\begin{aligned}
I_1 &= \frac{F_D D_{sat,D} (1-E)}{1-D_{sat,D} E} + F_A A_{sat,A} S_4 + \frac{(1-A_{sat,D}) F_D D_{sat,D} E \alpha_{sat} S_4}{(1-D_{sat,D} E) S_2} \\
I_2 &= \frac{F_D D_{sat,D} (1-E)}{1-D_{sat,D} E} S_1 + F_A A_{sat,A} S_2 + \frac{(1-A_{sat,D}) F_D D_{sat,D} E \alpha_{sat}}{(1-D_{sat,D} E)} \\
I_3 &= \frac{F_D D_{sat,D} (1-E)}{1-D_{sat,A} E} S_3 + F_A A_{sat,A} + \frac{A_{sat,D} (1-A_{sat,A}) F_D D_{sat,A} E \alpha_{sat}}{A_{sat,A} (1-D_{sat,A} E)} \frac{1}{S_2}
\end{aligned} \tag{S27}$$

where

$$\begin{aligned}
F_D &= D_{all} k_{f,D} \eta_{D,1} \\
F_A &= A_{All} k_{f,A} \eta_{A,3}
\end{aligned} \tag{S28}$$

The unquenched donor (I_D) and directly-excited acceptor intensities (I_A) are related to F_D and F_A according to the following equations:

$$\begin{aligned}
I_D &= F_D D_{sat,D} \\
I_A &= F_A A_{sat,A}
\end{aligned} \tag{S29}$$

The equation is quadratic in E , and the meaningful roots for E , I_D and I_A are too long to be presented here, but provided in the “fretWithSat_1.m” file (available at the end of this PDF).

If the ratio of the donor and the acceptor is known and constant for every pixel (e.g. when FRET between a donor and acceptor present in a fusion construct is measured), equation set (S27) can be supplementing with a fourth equation enabling the simultaneous determination of α and the FRET efficiency²:

$$\alpha_{sat} = \frac{I_A S_2 R_{exp} D_{sat,D} \tau_A}{I_D A_{sat,D} \tau_D} \tag{S30}$$

where R_{exp} is the ratio of the number of donors to acceptors. The meaningful roots of this quadratic equation set are provided in the fretWithSat_2.m file.

Determination of the FRET efficiency considering donor saturation and FRET frustration in an intensity-based experiment

An excited acceptor cannot serve as an acceptor for an excited donor. The effect of this phenomenon, usually called frustrated FRET, was taken into account by considering a system consisting of one donor and one acceptor. The equilibrium for the four different molecular species in the system (DA – ground-state donor and acceptor; D^{*}A – excited donor and ground-state acceptor; DA^{*} – ground-state donor and excited acceptor; D^{*}A^{*} – excited donor and acceptor) is described by the following matrix equation:

$$\begin{pmatrix} 0 \\ 0 \\ 0 \\ 0 \\ DA_{all} \end{pmatrix} = \begin{pmatrix} -\Phi(\sigma_D + \sigma_A) & \frac{1}{\tau_D} & \frac{1}{\tau_A} & 0 \\ \Phi \sigma_D & -\frac{1}{(1-E)\tau_D} - \Phi \sigma_A & 0 & \frac{1}{\tau_A} \\ \Phi \sigma_A & \frac{E}{(1-E)\tau_D} & -\frac{1}{\tau_A} - \Phi \sigma_D & \frac{1}{\tau_D} \\ 0 & \Phi \sigma_A & \Phi \sigma_D & -\left(\frac{1}{\tau_D} + \frac{1}{\tau_A}\right) \\ 1 & 1 & 1 & 1 \end{pmatrix} \begin{pmatrix} DA \\ D^*A \\ DA^* \\ D^*A^* \end{pmatrix} \quad (S31)$$

whose solution is provided below:

$$\begin{aligned} DA &= \frac{DA_{all}(-\tau_D + \tau_A(-1 + (E-1)(\sigma_A + \sigma_D)\tau_D \Phi))}{\tau_D(-1 + (E-1)\sigma_D \tau_D \Phi) + \tau_A^2 \Phi(1 + \sigma_D \tau_D \Phi)(-\sigma_A - E \sigma_D + (E-1)\sigma_A(\sigma_A + \sigma_D)\tau_D \Phi) + \tau_A(-1 + \tau_D \Phi((E-2)(\sigma_A + \sigma_D) + (E-1)\sigma_D(2\sigma_A + \sigma_D)\tau_D \Phi))} \\ D^*A &= \frac{DA_{all}(E-1)\sigma_D \tau_D \Phi(\tau_A + \tau_D + (\sigma_A + \sigma_D)\tau_A \tau_D \Phi)}{\tau_D(-1 + (E-1)\sigma_D \tau_D \Phi) + \tau_A^2 \Phi(1 + \sigma_D \tau_D \Phi)(-\sigma_A - E \sigma_D + (E-1)\sigma_A(\sigma_A + \sigma_D)\tau_D \Phi) + \tau_A(-1 + \tau_D \Phi((E-2)(\sigma_A + \sigma_D) + (E-1)\sigma_D(2\sigma_A + \sigma_D)\tau_D \Phi))} \\ DA^* &= \frac{DA_{all} \tau_A \Phi(-(\sigma_A + E \sigma_D)(\tau_A + \tau_D) + (E-1)\sigma_A(\sigma_A + \sigma_D)\tau_A \tau_D \Phi)}{\tau_D(-1 + (E-1)\sigma_D \tau_D \Phi) + \tau_A^2 \Phi(1 + \sigma_D \tau_D \Phi)(-\sigma_A - E \sigma_D + (E-1)\sigma_A(\sigma_A + \sigma_D)\tau_D \Phi) + \tau_A(-1 + \tau_D \Phi((E-2)(\sigma_A + \sigma_D) + (E-1)\sigma_D(2\sigma_A + \sigma_D)\tau_D \Phi))} \\ D^*A^* &= \frac{DA_{all} \sigma_D \tau_A \tau_D \Phi^2(-\sigma_A \tau_A - E \sigma_D \tau_A - \sigma_A \tau_D + E \sigma_A \tau_D + (E-1)\sigma_A(\sigma_A + \sigma_D)\tau_A \tau_D \Phi)}{\tau_D(-1 + (E-1)\sigma_D \tau_D \Phi) + \tau_A^2 \Phi(1 + \sigma_D \tau_D \Phi)(-\sigma_A - E \sigma_D + (E-1)\sigma_A(\sigma_A + \sigma_D)\tau_D \Phi) + \tau_A(-1 + \tau_D \Phi((E-2)(\sigma_A + \sigma_D) + (E-1)\sigma_D(2\sigma_A + \sigma_D)\tau_D \Phi))} \end{aligned} \quad (S32)$$

If complexes of one donor and one acceptor are considered in the model, the number of donors and acceptors is equal significantly limiting the applicability of the method. In order to increase the flexibility of the model, free donors, free acceptor or both should also be considered. Measurement of three independent intensities (I_1 , I_2 , I_3) allows for the determination of three unknowns: 1. the concentration of the donor-acceptor complex; 2. the FRET efficiency; and

3. either the concentration of free donors or free acceptors. Free donors are typically disregarded in intensity-based FRET measurements in which the FRET efficiency is determined without explicitly calculating the fraction of complexed donors. This simplification results in an apparent decrease in the calculated FRET efficiency. In order to maintain comparability between this new approach and previous intensity-based methods free acceptors (A_f) were considered in the model in order to uncouple the number of donors and acceptors from each other. Using an approach similar to the one used for equation (S27) let us write the donor and acceptor intensities in channels I_1 - I_3 :

$$\begin{aligned}
I_{D,1} &= D^*A^* k_{f,D} \eta_{D,1} + D^*A k_{f,D} \eta_{D,1} \\
I_{A,1} &= (D^*A^* + DA^*) k_{f,A} \eta_{A,1} + A_f \frac{\sigma_{A(D)} \tau_A \Phi_D}{1 + \sigma_{A(D)} \tau_A \Phi_D} k_{f,A} \eta_{A,1} \\
I_{D,2} &= D^*A^* k_{f,D} \eta_{D,2} + D^*A k_{f,D} \eta_{D,2} \\
I_{A,2} &= (D^*A^* + DA^*) k_{f,A} \eta_{A,2} + A_f \frac{\sigma_{A(D)} \tau_A \Phi_D}{1 + \sigma_{A(D)} \tau_A \Phi_D} k_{f,A} \eta_{A,2} \\
I_{D,3} &= D^*A^* k_{f,D} \eta_{D,3} + D^*A k_{f,D} \eta_{D,3} \\
I_{A,3} &= (D^*A^* + DA^*) k_{f,A} \eta_{A,3} + A_f \frac{\sigma_A \tau_A \Phi_A}{1 + \sigma_A \tau_A \Phi_A} k_{f,A} \eta_{A,3} \\
I_D &= DA_{all} k_{f,D} \eta_{D,1} \\
I_A &= (DA_{all} + A_f) k_{f,A} \eta_{A,3}
\end{aligned} \tag{S33}$$

where $I_{D,X}$ and $I_{A,X}$ are the fluorescence intensities of the donor and the acceptor, respectively, in fluorescence channel X ($X=1,2,3$ corresponding to the donor, FRET and acceptor channels), $k_{f,D}$ and $k_{f,A}$ are the rate constants of fluorescence of the donor and acceptor, respectively, and $\eta_{D,X}$ and $\eta_{A,X}$ are the detection efficiencies of donor and acceptor photons, respectively, in the X^{th} fluorescence channel. The equilibrium population densities of D^*A^* , D^*A and DA^* are obtained from equation (S32) followed by solving for $I_{D,X}$ and $I_{A,X}$. The solutions are too long to be presented here. Using these analytical solutions an equation set was written for the measured I_1 - I_3 intensities:

$$\begin{aligned}
I_1 &= I_{D,1} + I_{A,1} \\
I_2 &= I_{D,2} + I_{A,2} \\
I_3 &= I_{D,3} + I_{A,3}
\end{aligned} \tag{S34}$$

A numerical solution for this cubic equation set was found in Matlab. Roots in which I_D , I_A and E were all positive were selected as the meaningful solution. The Matlab file is available at the end of this PDF (fretWithSatFrust_1.m).

Equation set (S33) was also written for a FRET pair consisting of one donor and one acceptor, i.e. in the absence of free acceptors. A numerical solution to this equation set was found in a similar way as for the general case containing free acceptors as well (fretWithSatFrust_2.m).

SUPPLEMENTARY REFERENCES

- 1 Trón, L. *et al.* Flow cytometric measurement of fluorescence resonance energy transfer on cell surfaces. Quantitative evaluation of the transfer efficiency on a cell-by-cell basis. *Biophys J* **45**, 939-946 (1984).
- 2 Szalóki, N. *et al.* High throughput FRET analysis of protein-protein interactions by slide-based imaging laser scanning cytometry. *Cytometry A* **83**, 818-829, doi:10.1002/cyto.a.22315 (2013).

SUPPLEMENTARY FIGURES

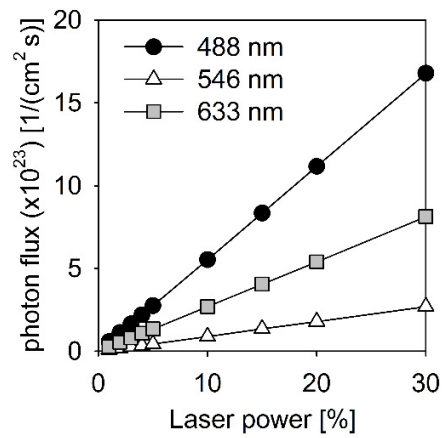


Figure S1. Measurement of photon flux. The intensity of the three laser lines were adjusted on a percent scale shown on the horizontal axis. The physical power at the focal plane was measured followed by converting it to photon flux.

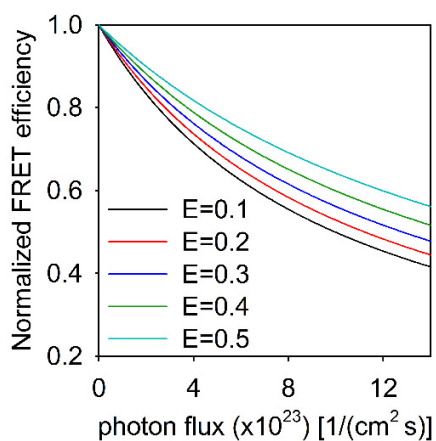


Figure S2. Dependence of the FRET efficiency calculated according to the conventional method on the photon flux and the theoretical FRET efficiency. A donor characterized by a fluorescence lifetime of 4.1 ns and a molar absorption coefficient of $71,000 \text{ M}^{-1}\text{cm}^{-1}$, corresponding to AlexaFluor488, was assumed to undergo energy transfer characterized by FRET efficiencies ranging from 0.1 to 0.5. The apparent FRET efficiency was calculated from donor quenching according to equation (S7) assuming no intersystem crossing to the triplet state, and it was normalized to the theoretical values measurable at infinitesimally low excitation power.

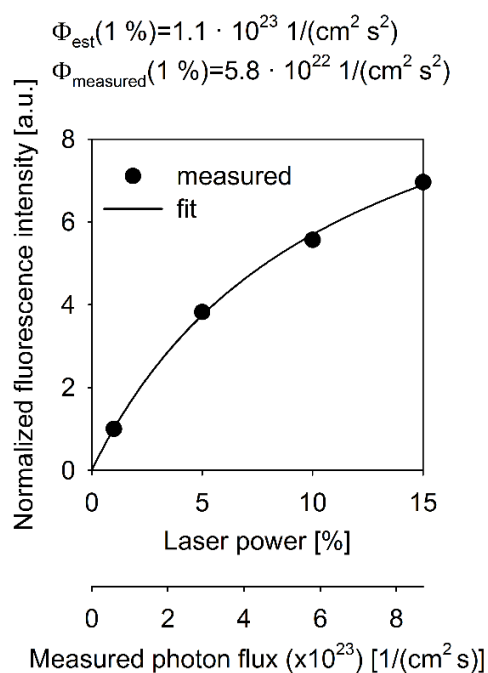


Figure S3. Determination of the apparent photon flux from fluorophore saturation. The fluorescence intensity of a 50 nM solution of AlexaFluor488 carboxylic acid was measured in a plane adjacent to the coverslip at four different laser intensities corresponding to 1%, 5%, 10% and 15% laser powers adjusted on the microscope. The fluorescence intensities were normalized to the value measured at 1% laser power followed by fitting equation (S19) to the normalized intensities. Fitting provided the apparent, estimated photon flux (Φ_{est}), which is approximately two-times higher than the real, measured photon flux also shown above the figure. The horizontal scale of the figure displays the laser power on a percent scale as adjusted on the microscope as well as the photon flux measured by an optical power meter.

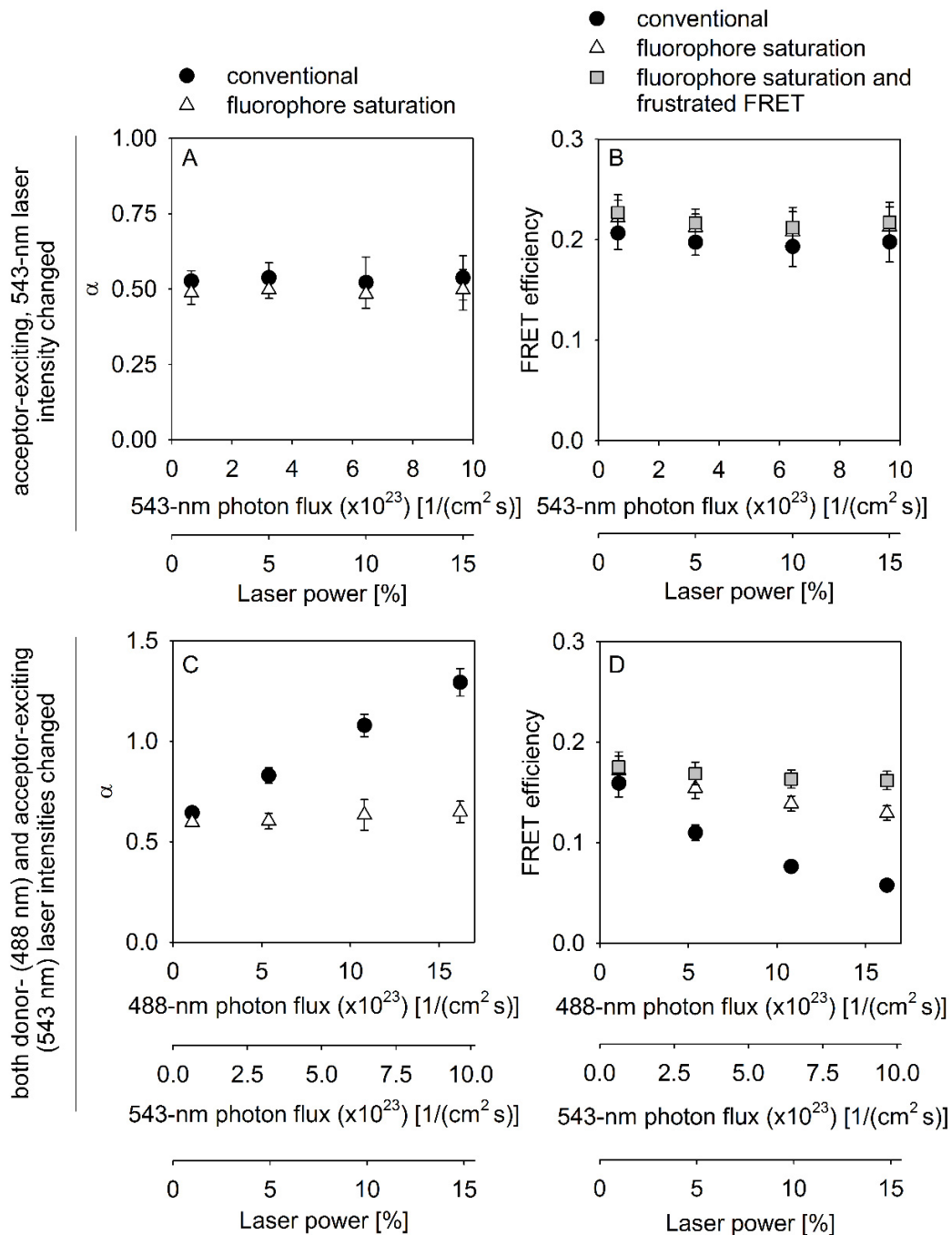


Figure S4. Dependence of parameter α and the apparent FRET efficiency on the intensity of the donor- and acceptor-exciting lasers. (A) SKBR-3 cells were labeled with AlexaFluor488-trastuzumab or AlexaFluor546-trastuzumab, and the fluorescence intensities of both the donor- and the acceptor-labeled samples were measured in the donor and FRET channels, respectively,

at different intensities of the 543-nm laser while holding the photon flux of the 488-nm laser at a constant value of $5.8 \cdot 10^{22} \text{ 1/(cm}^2 \text{ s)}$ corresponding to a laser power of 1%. Parameter α was determined according to the conventional approach disregarding fluorophore saturation (equation (S23)) and using the proposed method considering saturation phenomena (equation (S24)). (B) Cells were labeled with both AlexaFluor488-trastuzumab and AlexaFluor546-pertuzumab and intensities were measured in the donor, FRET and acceptor channels at different intensities of the 543-nm laser while holding the photon flux of the 488-nm laser at a constant value of $5.8 \cdot 10^{22} \text{ 1/(cm}^2 \text{ s)}$ corresponding to a laser power of 1%. FRET was evaluated in three different ways: conventional disregarding saturation phenomena (●), considering donor saturation (Δ) and considering both donor saturation and FRET frustration (■). (C-D) The same samples were measured and analyzed as in parts A and B, but both the 488-nm and 543-nm laser intensities were changed as shown on the horizontal axes.

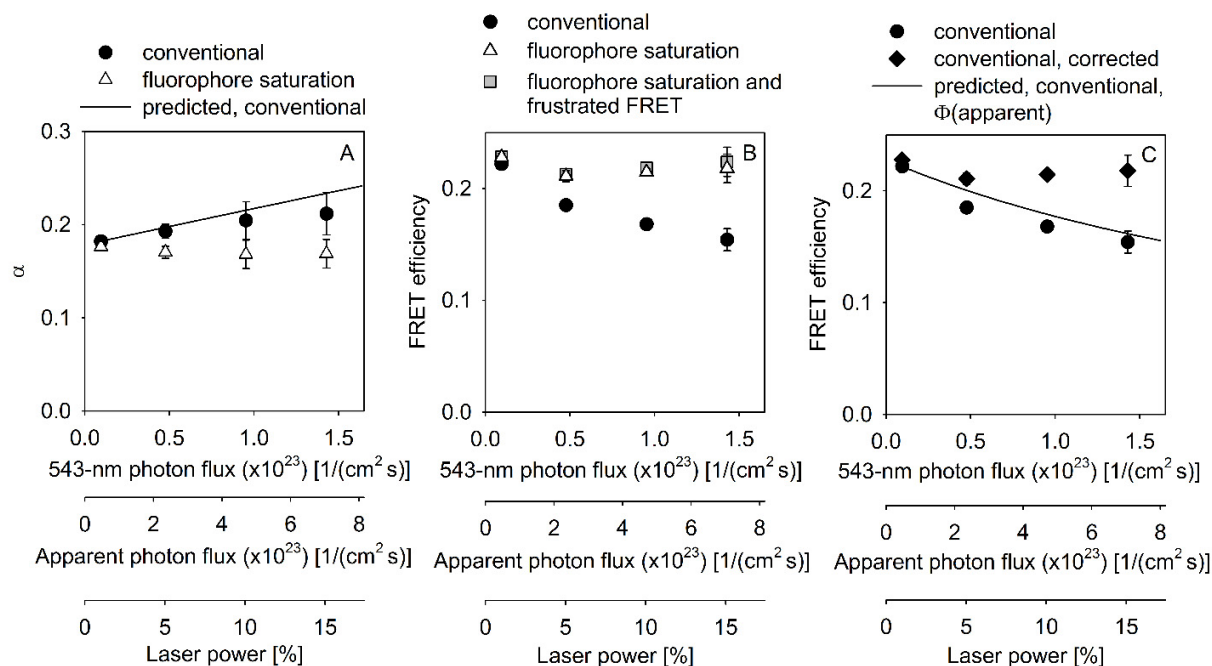


Figure S5. Evaluation of FRET in the AlexaFluor546-AlexaFluor647 donor-acceptor system. (A) SKBR-3 cells were labeled with AlexaFluor546-trastuzumab or AlexaFluor647-trastuzumab, and the fluorescence intensities of both the donor- and the acceptor-labeled samples were measured in the donor and FRET channels, respectively, at different intensities of the 543-nm laser. Parameter α was determined according to the conventional approach disregarding fluorophore saturation (equation (S23)) and using the proposed method considering saturation phenomena (equation (S24)). The continuous line shows the predicted dependence of α , calculated in the conventional way, on excitation intensity (equation (S26)). The real photon flux, the apparent photon flux (equation (S20)) and the relative intensity on a percent scale, as adjusted on the microscope, are displayed on the horizontal axes in both parts of the figure. (B-C) Cells were labeled with both AlexaFluor546-trastuzumab and AlexaFluor633-pertuzumab and intensities were measured in the donor, FRET and acceptor channels at different intensities of the 543-nm laser. FRET was evaluated in four different ways: conventional disregarding saturation phenomena (●), considering donor saturation (△), considering both donor saturation and FRET frustration (■), and conventional calculation corrected for donor saturation according to equation (S8) (◆). The FRET values are shown in two different figures because otherwise the symbols corresponding to the calculation methods considering saturation phenomena would overlap each other. The continuous line shows how the FRET efficiency calculated according to the conventional approach is expected to decline as a function of the apparent photon flux according to equation (S7). The photon flux of the acceptor-exciting, 633-nm laser was $2.9 \cdot 10^{22}$ 1/(cm² s) corresponding to a laser power of 1%.

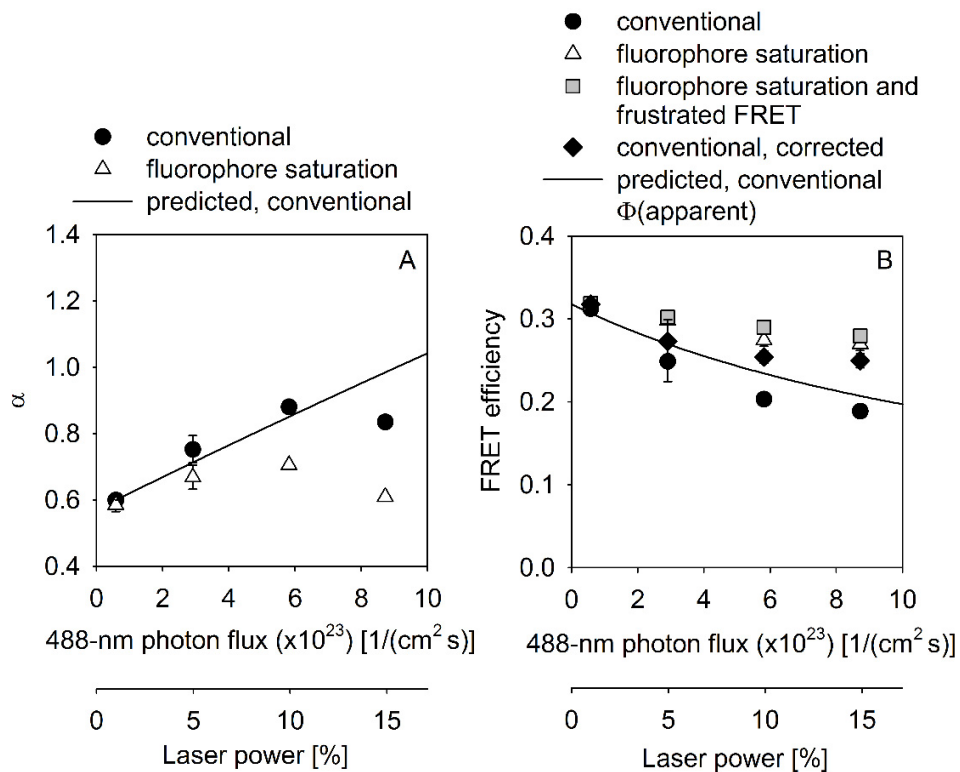


Figure S6. Evaluation of FRET in the mCherry-GFP donor-acceptor system. (A) Cells were transfected with an mCherry-GFP plasmid leading to the production of a protein containing both fluorescent proteins. The fluorescence intensities were measured at different intensities of the 488-nm laser, and parameter α was determined according to equation (S23) (disregarding fluorophore saturation) and equation (S24) (considering fluorophore saturation). The continuous line shows the predicted dependence of α , calculated in the conventional way, on excitation intensity (equation (S26)). The real photon flux and the relative intensity on a percent scale, as adjusted on the microscope, are displayed on the horizontal axes in both parts of the figure. The apparent photon flux is not shown since it was determined to be identical to the real photon flux. (B) The fluorescence intensity of cells transfected with the mCherry-GFP construct was measured in the donor, FRET and acceptor channels at different intensities of the 488-nm laser. FRET was evaluated in four different ways: conventional disregarding saturation phenomena (●), considering donor saturation (△), considering both donor saturation and FRET frustration (■), and conventional calculation corrected for donor saturation according to equation (S8) (◆). The continuous line shows how the FRET efficiency calculated according to the conventional approach is expected to decline as a function of the photon flux according to equation (S7). The photon flux of the acceptor-exciting, 543-nm laser was $9.5 \cdot 10^{21}$ $1/(\text{cm}^2 \text{ s})$ corresponding to a laser power of 1%.

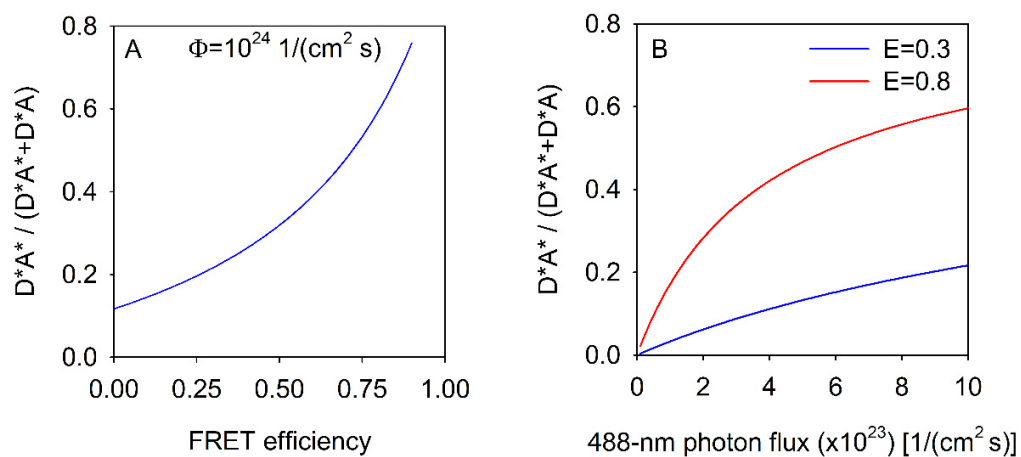


Figure S7. Complexes of excited donors and excited acceptors (D^*A^*) are hardly present at low FRET efficiencies. A complex of AlexaFluor488 and AlexaFluor546 excited at 488 nm was simulated according to equation (S32). The fraction of D^*A^* among complexes containing excited donors ($D^*A^* + D^*A$) is plotted on the vertical axes. The fractional presence of D^*A^* strongly depends on the FRET efficiency at a constant photon flux (A). The excitation power-dependent accumulation of D^*A^* at two different FRET values also shows that such doubly-excited species is negligibly present at low FRET efficiencies (B).

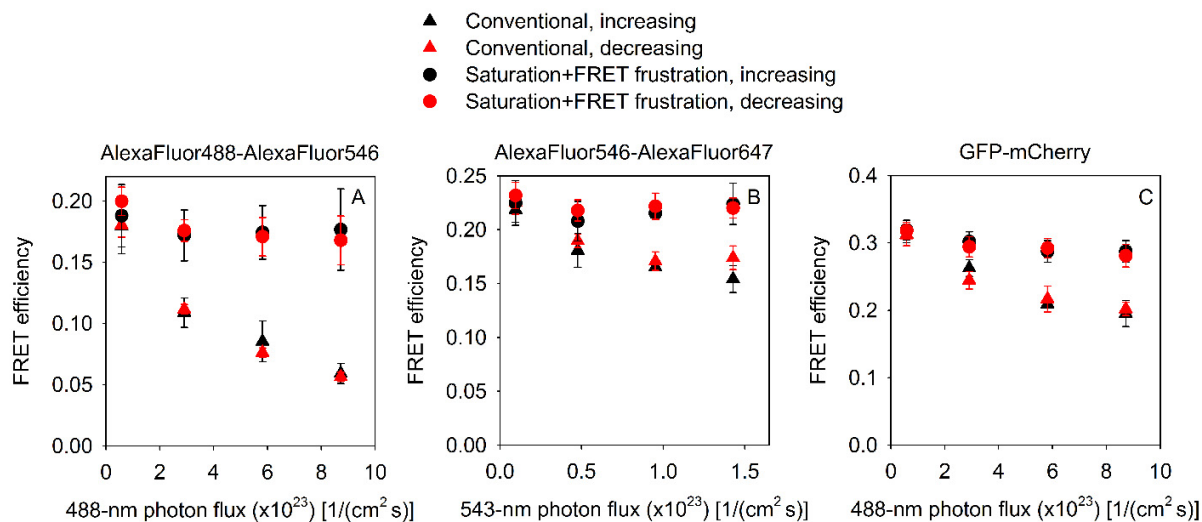


Figure S8. Lack of photobleaching-induced distortion in the FRET measurements using three different donor-acceptor pairs. FRET taking place in the three different experimental systems used throughout the manuscript was measured using the conventional approach uncorrected for saturation phenomena (triangles) and correcting for fluorophore saturation and FRET frustration (circles). The experiments were carried out at four different donor excitation intensities, while holding the acceptor intensity constant. The measurements were performed in two different ways. The excitation power was gradually increased in an image (black symbols), while it was gradually decreased in another one (red symbols). The mean \pm SEM of three such measurement pairs is presented in the figure.

TEXT VERSIONS OF MATLAB FILES

```
function
[fret,id,ia]=fretWithSat_1(i1,i2,i3,S1,S2,S3,S4,alphaSat,tauD,tauA,sigmaD,sigmaDa,sigmaA,sigmaAd,phiD,phiA)
% This function takes the saturation of donor and acceptor fluorescence
% into consideration, but neglects FRET frustration as a result of acceptor
% saturation.
%
% i1,i2,i3 - intensities measured in the donor, FRET and acceptor channel,
% respectively
% S1,S2,S3,S4 - overspill parameters
% alphaSat,alphaClassic - parameter alpha calculated considering and
% disregarding fluorophore saturation, respectively
% tauD,tauA - fluorescence lifetime of the donor and acceptor, respectively
% sigmaD,sigmaDa - absorption cross-section of the donor at the donor and
% acceptor excitation wavelength, respectively
% sigmaA,sigmaAd - absorption cross-section of the acceptor at the acceptor
% and donor excitation wavelength, respectively
% phiD,phiA - photon flux of the donor- and acceptor-exciting laser,
% respectively
%
% fret,id,ia - solutions (FRET efficiency, unquenched donor intensity,
% directly-excited acceptor intensity)
%
% Dsat0d - fractional saturation of the donor at the donor excitation
% wavelength
% Dsat0a - fractional saturation of the donor at the acceptor excitation
% wavelength
% Asat0a - fractional saturation of the acceptor at the acceptor excitation
% wavelength
% Asat0d - fractional saturation of the acceptor at the donor excitation
% wavelength
%
% Peter Nagy, email: peter.v.nagy@gmail.com
Dsat0d=sigmaD.*tauD.*phiD.*(1+sigmaD.*tauD.*phiD).^(-1);
Dsat0a=sigmaDa.*tauD.*phiA.*(1+sigmaDa.*tauD.*phiA).^(-1);
Asat0d=sigmaAd.*tauA.*phiD.*(1+sigmaAd.*tauA.*phiD).^(-1);
Asat0a=sigmaA.*tauA.*phiA.*(1+sigmaA.*tauA.*phiA).^(-1);
fret=(1/2).*Dsat0d.^(-1).*(Asat0a.*S2.*(Dsat0d.*S3.*(i1.*S2+(-
1).*i2.*S4)+Dsat0a.*(i2+(-1).*i1.*S1+(-1).*i3.*S2+i3.*S1.*S4)))+(Asat0a+(-
1).*Asat0d).*Dsat0a.*(i1.*S2+(-1).*i2.*S4).*alphaSat).^(-1).*(Asat0d.*((-
1)+Asat0a).*Dsat0a+(-1).*Asat0a.*Dsat0d).*(i1.*S2+(-1).*i2.*S4).*alphaSat+(-
1).*((-4).*Asat0a.*Dsat0d.^2.*S2.*(i1.*(S1+(-1).*S2.*S3)+i3.*(S2+(-
1).*S1.*S4)+i2.*((-1)+S3.*S4)).*(Asat0a.*S2.*(Dsat0d.*S3.*((-
1).*i1.*S2+i2.*S4)+Dsat0a.*((-1).*i2+i1.*S1+i3.*S2+(-1).*i3.*S1.*S4)))+( (-
1).*Asat0a+Asat0d).*Dsat0a.*(i1.*S2+(-
1).*i2.*S4).*alphaSat)+(Asat0a.*Dsat0d.*S2.*((-1)+(-
1).*Dsat0a).*i2+(1+Dsat0a).*i1.*S1+(-
1).**(1+Dsat0d).*i1.*S2.*S3+(1+Dsat0d).*i2.*S3.*S4+(1+Dsat0a).*i3.*(S2+(-
1).*S1.*S4)))+(1+(-1).*Asat0a).*Asat0d.*Dsat0a+Asat0a.*((-
1)+Asat0d).*Dsat0d).*(i1.*S2+(-
1).*i2.*S4).*alphaSat).^2).^^(1/2)+Asat0a.*Dsat0d.*(i2.*S2.*(1+Dsat0a+(-
1).**(1+Dsat0d).*S3.*S4)+(-1).*i2.*S4.*alphaSat+S2.*((1+Dsat0a).*i3.*((-
1).*S2+S1.*S4)+i1.*((-1)+(-1).*Dsat0a).*S1+(1+Dsat0d).*S2.*S3+alphaSat)))));
fd=(1/2).*Dsat0d.^(-1).*(Asat0a.*Asat0d.*Dsat0d+Asat0a.*((-
1)+Dsat0a).*Dsat0d+(-1).*Asat0d.*Dsat0a.*((-1)+Asat0a+Dsat0d)).^(-1).*(S2+(-
```



```

1)+Asat0d).*Dsat0d).*(i1.*S2+(-1).*i2.*S4).*alphaSat).^2).^^(1/2)+(-
1).*Asat0d.*((-4).*Asat0a.*Dsat0d.^2.*S2.*(i1.*(S1+(-1).*S2.*S3)+i3.*(S2+(-
1).*S1.*S4)+i2.*((-1)+S3.*S4)).*(Asat0a.*S2.*(Dsat0d.*S3.*((-
1).*i1.*S2+i2.*S4)+Dsat0a.*((-1).*i2+i1.*S1+i3.*S2+(-1).*i3.*S1.*S4)))+((-
1).*Asat0a+Asat0d).*Dsat0a.*(i1.*S2+(-
1).*i2.*S4).*alphaSat)+(Asat0a.*Dsat0d.*S2.*((-1)+(-
1).*Dsat0a).*i2+(1+Dsat0a).*i1.*S1+(-
1).(1+Dsat0d).*i1.*S2.*S3+(1+Dsat0d).*i2.*S3.*S4+(1+Dsat0a).*i3.*(S2+(-
1).*S1.*S4)))+(1+(-1).*Asat0a).*Asat0d.*Dsat0a+Asat0a.*((-
1)+Asat0d).*Dsat0d).*(i1.*S2+(-1).*i2.*S4).*alphaSat).^2).^^(1/2));
id=fd.*Dsat0d;
ia=fa.*Asat0a;

```

```

function
[fret,alpha,id,ia]=fretWithSat_2(i1,i2,i3,expRat,S1,S2,S3,S4,tauD,tauA,sigmaD,
sigmaDa,sigmaA,sigmaAd,phiD,phiA)
% This function takes the saturation of donor and acceptor fluorescence
% into consideration, but neglects FRET frustration as a result of acceptor
saturation.
% It calculates both E and alpha when the donor-acceptor ratio is known.
%
% i1,i2,i3 - intensities measured in the donor, FRET and acceptor channel,
respectively
% expRat - the ratio of the number of donors to acceptors
% S1,S2,S3,S4 - overspill parameters
% tauD,tauA - fluorescence lifetime of the donor and acceptor, respectively
% sigmaD,sigmaDa - absorption cross-section of the donor at the donor and
acceptor excitation wavelength, respectively
% sigmaA,sigmaAd - absorption cross-section of the acceptor at the acceptor
and donor excitation wavelength, respectively
% phiD,phiA - photon flux of the donor- and acceptor-exciting laser,
respectively
%
% fret,alpha,id,ia - solutions for the FRET efficiency, alpha, unquenched
% donor fluorescence and directly-excited acceptor fluorescence
%
% Dsat0d - fractional saturation of the donor at the donor excitation
wavelength
% Dsat0a - fractional saturation of the donor at the acceptor excitation
wavelength
% Asat0a - fractional saturation of the acceptor at the acceptor excitation
wavelength
% Asat0d - fractional saturation of the acceptor at the donor excitation
wavelength
%
% Peter Nagy, email: peter.v.nagy@gmail.com

Dsat0d=sigmaD.*tauD.*phiD.*(1+sigmaD.*tauD.*phiD).^(-1);
Dsat0a=sigmaDa.*tauD.*phiA.*(1+sigmaDa.*tauD.*phiA).^(-1);
Asat0d=sigmaAd.*tauA.*phiD.*(1+sigmaAd.*tauA.*phiD).^(-1);
Asat0a=sigmaA.*tauA.*phiA.*(1+sigmaA.*tauA.*phiA).^(-1);

fret=(1/2).*Dsat0d.^(-1).*(expRat.*(Asat0a.*Asat0d.*Dsat0d.*S3.*(i1.* ...
S2+(-1).*i2.*S4)+Asat0a.*Dsat0d.*S3.*((-1).*i1.*S2+i2.*S4)+ ...
Asat0a.*Dsat0a.*i3.*(S2+(-1).*S1.*S4)+Asat0d.*Dsat0a.*((-1)+ ...
Asat0a).*i2+i1.*(S1+(-1).*Asat0a.*S1)+Asat0a.*i3.*((-1).*S2+S1.* ...
S4)).*tauA+Asat0a.*Asat0d.*(Dsat0d.*S3.*(i1.*S2+(-1).*i2.*S4)+ ...
Dsat0a.*(i2+(-1).*i1.*S1+(-1).*i3.*S2+i3.*S1.*S4)).*tauD).^(-1).*( ...
Asat0a.*Dsat0d.*expRat.*((-1).*i1.*S2.*S3+i2.*S3.*S4+i3.*(S2+(-1) ...
.*S1.*S4)).*tauA+Asat0d.*expRat.*((-1)+Asat0a).*Dsat0a.*(i2+(-1).* ...
i1.*S1)+Asat0a.*Dsat0d.*((-1).*i3.*S2+i1.*S2.*S3+i3.*S1.*S4+(-1).* ...
i2.*S3.*S4)).*tauA+Asat0a.*Asat0d.*(Dsat0a.*(i2+(-1).*i1.*S1+(-1).* ...
i3.*S2+i3.*S1.*S4)+Dsat0d.*(i2+(-1).*i1.*S1+(-1).*i3.*S2+2.*i1.* ...
S2.*S3+i3.*S1.*S4+(-2).*i2.*S3.*S4)).*tauD+(-1).*(Asat0a.*Dsat0d.* ...
expRat.*((-1).*i1.*S2.*S3+i2.*S3.*S4+i3.*(S2+(-1).*S1.*S4)).*tauA+ ...
Asat0d.*expRat.*((-1)+Asat0a).*Dsat0a.*(i2+(-1).*i1.*S1)+Asat0a.* ...
Dsat0d.*((-1).*i3.*S2+i1.*S2.*S3+i3.*S1.*S4+(-1).*i2.*S3.*S4)).* ...
tauA+Asat0a.*Asat0d.*(Dsat0a.*(i2+(-1).*i1.*S1+(-1).*i3.*S2+i3.*S1.* ...
S4)+Dsat0d.*(i2+(-1).*i1.*S1+(-1).*i3.*S2+2.*i1.*S2.*S3+i3.*S1.* ...
S4+(-2).*i2.*S3.*S4)).*tauD).^2+(-4).*Asat0a.*Asat0d.*Dsat0d.*(i1.*( ...

```

```

S1+(-1).*S2.*S3)+i3.*(S2+(-1).*S1.*S4)+i2.*((-1)+S3.*S4)).*tauD.*( ...
Asat0a.*expRat.*(Dsat0d.*S3.*(i1.*S2+(-1).*i2.*S4)+Dsat0a.*i3.*(( ...
-1).*S2+S1.*S4)).*tauA+Asat0d.*(Dsat0a.*expRat.*(i2+(-1).*Asat0a.* ...
i2+((-1)+Asat0a).*i1.*S1+Asat0a.*i3.*(S2+(-1).*S1.*S4)).*tauA+ ...
Asat0a.*Dsat0a.*((-1).*i2+i1.*S1+i3.*(S2+(-1).*S1.*S4)).*tauD+(-1).* ...
Asat0a.*Dsat0d.*S3.*(i1.*S2+(-1).*i2.*S4).*(expRat.*tauA+tauD))).^( ...
1/2));
fd=(1/2).*Dsat0d.^(-1).* (i1.*S2+(-1).*i2.*S4).*(S2+(-1).*S1.*S4).^( ...
-1).* (Asat0a.*Dsat0d.*expRat.*((1+(-1).*Dsat0d).*S3.*(i1.*S2+(-1) ...
.*i2.*S4)+((-1)+Dsat0a).*i3.*(S2+(-1).*S1.*S4)).*tauA+Asat0d.*( ...
Asat0a.*Dsat0d.*expRat.*((-1)+Dsat0d).*S3.*(i1.*S2+(-1).*i2.*S4)+ ...
i3.*(S2+(-1).*S1.*S4)).*tauA+Dsat0a.*expRat.*((-1)+Asat0a).*((-1)+ ...
Dsat0d).*i2+((-1)+Asat0a+Dsat0d+(-1).*Asat0a.*Dsat0d).*i1.*S1+ ...
Asat0a.*Dsat0d.*i3.*((-1).*S2+S1.*S4)).*tauA+Asat0a.*Dsat0a.*((-1)+ ...
Dsat0d).* (i2+(-1).*i1.*S1+(-1).*i3.*S2+i3.*S1.*S4).*tauD+Asat0a.*(( ...
-1)+Dsat0d).* (i1.*(S1+((-1)+Dsat0d).*S2.*S3)+i3.*(S2+(-1).*S1.*S4) ...
+i2.*((-1)+S3.*(S4+(-1).*Dsat0d.*S4))).*tauD)).^(-1).* (Asat0a.* ...
Dsat0d.*expRat.*((1+(-1).*Dsat0d).*S3.*(i1.*S2+(-1).*i2.*S4)+((-1) ...
+2.*Dsat0a+(-1).*Dsat0d).*i3.*(S2+(-1).*S1.*S4)).*tauA+Asat0d.*( ...
Dsat0a.*expRat.*((-1)+Asat0a).*((-1)+Dsat0d).*i2+((-1)+Asat0a+ ...
Dsat0d+(-1).*Asat0a.*Dsat0d).*i1.*S1+(-2).*Asat0a.*Dsat0d.*i3.*( ...
S2+(-1).*S1.*S4)).*tauA+Asat0a.*Dsat0a.*((-1)+Dsat0d).* (i2+(-1).* ...
i1.*S1+(-1).*i3.*S2+i3.*S1.*S4).*tauD+Asat0a.*Dsat0d.* (expRat.*(( ...
-1)+Dsat0d).*S3.*(i1.*S2+(-1).*i2.*S4)+(1+Dsat0d).*i3.*(S2+(-1).* ...
S1.*S4)).*tauA+((-1)+Dsat0d).*((-1).*i2+i1.*S1+i3.*(S2+(-1).*S1.*S4) ...
).*tauD))+(-1).* ((Asat0a.*Dsat0d.*expRat.*((-1).*i1.*S2.*S3+i2.*S3.* ...
S4+i3.*(S2+(-1).*S1.*S4)).*tauA+Asat0d.*expRat.*((-1)+Asat0a).* ...
Asat0d.*expRat.*(((-1)+Asat0a).*Dsat0d.*expRat.*((-1).*i3.*S2+i1.*S2.* ...
S3+i3.*S1.*S4+(-1).*i2.*S3.*S4)).*tauA+Asat0a.*Asat0d.* (Dsat0a.* (i2+ ...
(-1).*i1.*S1+(-1).*i3.*S2+i3.*S1.*S4)+Dsat0d.* (i2+(-1).*i1.*S1+( ...
-1).*i3.*S2+2.*i1.*S2.*S3+i3.*S1.*S4+(-2).*i2.*S3.*S4)).*tauD).^2+( ...
-4).*Asat0a.*Asat0d.*Dsat0d.* (i1.*(S1+(-1).*S2.*S3)+i3.*(S2+(-1).* ...
S1.*S4)+i2.*((-1)+S3.*S4)).*tauD.*(Asat0a.*expRat.*(Dsat0d.*S3.*( ...
i1.*S2+(-1).*i2.*S4)+Dsat0a.*i3.*((-1).*S2+S1.*S4)).*tauA+Asat0d.*( ...
Dsat0a.*expRat.*(i2+(-1).*Asat0a.*i2+((-1)+Asat0a).*i1.*S1+ ...
Asat0a.*i3.*(S2+(-1).*S1.*S4)).*tauA+Asat0a.*Dsat0a.*((-1).*i2+i1.* ...
S1+i3.*(S2+(-1).*S1.*S4)).*tauD+(-1).*Asat0a.*Dsat0d.*S3.*(i1.*S2+( ...
-1).*i2.*S4).*(expRat.*tauA+tauD))).^(1/2)+Dsat0d.* ((Asat0a.*Dsat0d.* ...
expRat.*((-1).*i1.*S2.*S3+i2.*S3.*S4+i3.*(S2+(-1).*S1.*S4)).*tauA+ ...
Asat0d.*expRat.*(((-1)+Asat0a).*Dsat0a.* (i2+(-1).*i1.*S1)+Asat0a.* ...
Dsat0d.*((-1).*i3.*S2+i1.*S2.*S3+i3.*S1.*S4+(-1).*i2.*S3.*S4)).* ...
tauA+Asat0a.*Asat0d.* (Dsat0a.* (i2+(-1).*i1.*S1+(-1).*i3.*S2+i3.*S1.* ...
S4)+Dsat0d.* (i2+(-1).*i1.*S1+(-1).*i3.*S2+2.*i1.*S2.*S3+i3.*S1.* ...
S4+(-2).*i2.*S3.*S4)).*tauD).^2+(-4).*Asat0a.*Asat0d.*Dsat0d.* (i1.*( ...
S1+(-1).*S2.*S3)+i3.*(S2+(-1).*S1.*S4)+i2.*((-1)+S3.*S4)).*tauD.*( ...
Asat0a.*expRat.*(Dsat0d.*S3.*(i1.*S2+(-1).*i2.*S4)+Dsat0a.*i3.*(( ...
-1).*S2+S1.*S4)).*tauA+Asat0d.*(Dsat0a.*expRat.*(i2+(-1).*Asat0a.* ...
i2+((-1)+Asat0a).*i1.*S1+Asat0a.*i3.*(S2+(-1).*S1.*S4)).*tauA+ ...
Asat0a.*Dsat0a.*((-1).*i2+i1.*S1+i3.*(S2+(-1).*S1.*S4)).*tauD+(-1).* ...
Asat0a.*Dsat0d.*S3.*(i1.*S2+(-1).*i2.*S4).*(expRat.*tauA+tauD))).^( ...
1/2));
fa=(1/2).*Asat0a.^(-1).* (S2+(-1).*S1.*S4).^(1/2).*(((-1)+Asat0a).* ...
Asat0d.*Dsat0a+Asat0a.*Dsat0d+(-1).*Asat0a.*Asat0d.*Dsat0d).* ...
expRat.*tauA+Asat0a.*Asat0d.* (Dsat0a+(-1).*Dsat0d).*tauD).^(-1).* ( ...
Asat0a.*Dsat0d.*expRat.*((-1).*i1.*S2.*S3+i2.*S3.*S4+i3.*(S2+(-1) ...
.*S1.*S4)).*tauA+Asat0d.*expRat.*((-1)+Asat0a).*Dsat0a.* (i2+(-1).* ...
i1.*S1)+Asat0a.*Dsat0d.*((-1).*i3.*S2+i1.*S2.*S3+i3.*S1.*S4+(-1).* ...

```

```

i2.*S3.*S4)).*tauA+Asat0a.*Asat0d.*(Dsat0a+(-1).*Dsat0d).*(i2+i3.* ...
S2+(-1).*S1.*(i1+i3.*S4)).*tauD+((Asat0a.*Dsat0d.*expRat.*((-1).* ...
i1.*S2.*S3+i2.*S3.*S4+i3.*(S2+(-1).*S1.*S4)).*tauA+Asat0d.*expRat.*( ...
((-1)+Asat0a).*Dsat0a.*(i2+(-1).*i1.*S1)+Asat0a.*Dsat0d.*((-1).* ...
i3.*S2+i1.*S2.*S3+i3.*S1.*S4+(-1).*i2.*S3.*S4)).*tauA+Asat0a.* ...
Asat0d.*(Dsat0a.*(i2+(-1).*i1.*S1+(-1).*i3.*S2+i3.*S1.*S4)+ ...
Dsat0d.*(i2+(-1).*i1.*S1+(-1).*i3.*S2+2.*i1.*S2.*S3+i3.*S1.*S4+( ...
-2).*i2.*S3.*S4)).*tauD).^2+(-4).*Asat0a.*Asat0d.*Dsat0d.*(i1.*(S1+( ...
-1).*S2.*S3)+i3.*(S2+(-1).*S1.*S4)+i2.*((-1)+S3.*S4)).*tauD.*( ...
Asat0a.*expRat.*(Dsat0d.*S3.*(i1.*S2+(-1).*i2.*S4)+Dsat0a.*i3.*(( ...
-1).*S2+S1.*S4)).*tauA+Asat0d.*(Dsat0a.*expRat.*(i2+(-1).*Asat0a.* ...
i2+((-1)+Asat0a).*i1.*S1+Asat0a.*i3.*(S2+(-1).*S1.*S4)).*tauA+ ...
Asat0a.*Dsat0a.*((-1).*i2+i1.*S1+i3.*(S2+(-1).*S1.*S4)).*tauD+(-1).* ...
Asat0a.*Dsat0d.*S3.*(i1.*S2+(-1).*i2.*S4).*(expRat.*tauA+tauD))).^( ...
1/2));

```

```

id=fd.*Dsat0d;
ia=fa.*Asat0a;

```

```

alpha=ia./id.*S2.*expRat.*Dsat0d./Asat0d.*tauA./tauD;

```

```

function
[solutions,solutionsTable]=fretWithSatFrustr_1(i1num,i2num,i3num,S1num,S2num,S3
num,S4num,alphanum,tauDnum,tauAnum,sigmaDnum,sigmaDanum,sigmaAnum,sigmaAdnum,p
hiDnum,phiAnum)
% This function takes the saturation of donor and acceptor fluorescence and
% FRET frustration into consideration.
% Numerical solution for the Na<>Nd case (D-A complex + Afree).
%
% i1num,i2num,i3num - intensities measured in the donor, FRET and acceptor
channel, respectively
% S1num,S2num,S3num,S4num - overspill parameters
% alphanum - parameter alpha calculated CONSIDERING fluorophore saturation
% tauDnum,tauAnum - fluorescence lifetime of the donor and acceptor,
respectively
% sigmaDnum,sigmaDanum - absorption cross-section of the donor at the donor
and acceptor excitation wavelength, respectively
% sigmaAnum,sigmaAdnum - absorption cross-section of the acceptor at the
acceptor and donor excitation wavelength, respectively
% phiDnum,phiAnum - photon flux of the donor- and acceptor-exciting laser,
respectively
%
% solutions - structure variable containing the solutions (FRET efficiency,
unquenched donor (Id) and directly-excited acceptor (Ia) intensity)
% solutionsTable - summary of the solutions in table format
%
% Peter Nagy, email: peter.v.nagy@gmail.com
Dsat0dnum=sigmaDnum.*tauDnum.*phiDnum.*(1+sigmaDnum.*tauDnum.*phiDnum).^(-1);
Asat0anum=sigmaAnum.*tauAnum.*phiAnum.*(1+sigmaAnum.*tauAnum.*phiAnum).^(-1);

syms i1 i2 i3 S1 S2 S3 S4 Fd Fa fret tauD tauA phiD phiA sigmaD sigmaDa sigmaA
sigmaAd alphaSat
freteqs=[i1==Fa.*S4.*sigmaA.*tauA.*phiA.*(1+sigmaA.*tauA.*phiA).^(-1)+(-
1).*fret.*Fd.*S2.^(-1) ...
.*S4.*alphaSat.*sigmaD.*tauD.*phiD.*(1+sigmaAd.*tauA.*phiD).^(-
1).* (tauA+tauD+(sigmaAd+sigmaD).*tauA.* ...
tauD.*phiD).* (tauD.*((-1)+((-
1)+fret).*sigmaD.*tauD.*phiD)+tauA.^2.*phiD.*(1+sigmaD.* ...
tauD.*phiD).*((-1).*sigmaAd+(-1).*fret.*sigmaD+((-
1)+fret).*sigmaAd.*(sigmaAd+sigmaD).* ...
tauD.*phiD)+tauA.*((-1)+tauD.*phiD.*((-2)+fret).* (sigmaAd+sigmaD)+((-
1)+fret).*sigmaD.* ...
(2.*sigmaAd+sigmaD).*tauD.*phiD)).^(-1)+Fd.*sigmaD.*tauD.*phiD.*((-
1)+fret).*tauD+ ...
tauA.^2.*phiD.*((-1).*sigmaAd+(-1).*fret.*sigmaD+((-
1)+fret).*sigmaAd.*(sigmaAd+sigmaD).* ...
tauD.*phiD)+((-
1)+fret).*tauA.*(1+(2.*sigmaAd+sigmaD).*tauD.*phiD)).*(tauD.*((-1)+(( ...
-1)+fret).*sigmaD.*tauD.*phiD)+tauA.^2.*phiD.*(1+sigmaD.*tauD.*phiD)).*( (-
1).*sigmaAd+(-1) ...
.*fret.*sigmaD+((-1)+fret).*sigmaAd.*(sigmaAd+sigmaD).*tauD.*phiD)+tauA.*((-
1)+tauD.*phiD.* ( ...
((-2)+fret).* (sigmaAd+sigmaD)+((-
1)+fret).*sigmaD.*(2.*sigmaAd+sigmaD).*tauD.*phiD)).^( ...
-1);
i2==Fa.*S2.*sigmaA.*tauA.*phiA.*(1+sigmaA.*tauA.*phiA).^(-1)+(-
1).*fret.*Fd.*alphaSat.*sigmaD.* ...

```

```

tauD.*phiD.*(1+sigmaAd.*tauA.*phiD).^(-
1).*(tauA+tauD+(sigmaAd+sigmaD).*tauA.*tauD.*phiD).*(tauD.* ...
((-1)+((-
1)+fret).*sigmaD.*tauD.*phiD)+tauA.^2.*phiD.*(1+sigmaD.*tauD.*phiD).*(-1).*
...
sigmaAd+(-1).*fret.*sigmaD+((-
1)+fret).*sigmaAd.*(sigmaAd+sigmaD).*tauD.*phiD)+tauA.*((-1)+ ...
tauD.*phiD.*((-2)+fret).*(sigmaAd+sigmaD)+((-
1)+fret).*sigmaD.*(2.*sigmaAd+sigmaD).*tauD.* ...
phiD))).^(-1)+Fd.*S1.*sigmaD.*tauD.*phiD.*((-
1)+fret).*tauD+tauA.^2.*phiD.*((-1) ...
.*sigmaAd+(-1).*fret.*sigmaD+((-
1)+fret).*sigmaAd.*(sigmaAd+sigmaD).*tauD.*phiD)+((-1)+ ...
fret).*tauA.*(1+(2.*sigmaAd+sigmaD).*tauD.*phiD)).*(tauD.*((-1)+((-
1)+fret).*sigmaD.* ...
tauD.*phiD)+tauA.^2.*phiD.*(1+sigmaD.*tauD.*phiD).*(-1).*sigmaAd+(-
1).*fret.*sigmaD+((-1) ...
+fret).*sigmaAd.*(sigmaAd+sigmaD).*tauD.*phiD)+tauA.*((-1)+tauD.*phiD.*((-
2)+fret).*( ...
sigmaAd+sigmaD)+((-1)+fret).*sigmaD.*(2.*sigmaAd+sigmaD).*tauD.*phiD))).^(-
1);
i3==Fa.*sigmaA.*tauA.*phiA.*(1+sigmaA.*tauA.*phiA).^(-1)+(-
1).*fret.*Fd.*S2.^(-1).*alphaSat.* ...
sigmaA.^(-
1).*sigmaAd.*sigmaDa.*tauD.*(tauA+tauD+(sigmaA+sigmaDa).*tauA.*tauD.*phiA).*(t
auD.*((-1)+ ...
(-1)+fret).*sigmaDa.*tauD.*phiA)+tauA.^2.*phiA.*(1+sigmaDa.*tauD.*phiA).*(-
1).*sigmaA+ ...
-1).*fret.*sigmaDa+((-
1)+fret).*sigmaA.*(sigmaA+sigmaDa).*tauD.*phiA)+tauA.*((-1)+tauD.* ...
phiA.*((-2)+fret).*(sigmaA+sigmaDa)+((-
1)+fret).*sigmaDa.*(2.*sigmaA+sigmaDa).*tauD.*phiA) ...
).^(-1).*phiD.*(1+sigmaAd.*tauA.*phiD).^(-
1)+Fd.*S3.*sigmaD.*tauD.*(1+sigmaDa.*tauD.*phiA) ...
.*((-1)+fret).*tauD+tauA.^2.*phiA.*((-1).*sigmaA+(-1).*fret.*sigmaDa+((-1)+
...
fret).*sigmaA.*(sigmaA+sigmaDa).*tauD.*phiA)+((-
1)+fret).*tauA.*(1+(2.*sigmaA+sigmaDa).*tauD.* ...
phiA)).*(tauD.*((-1)+((-
1)+fret).*sigmaDa.*tauD.*phiA)+tauA.^2.*phiA.*(1+sigmaDa.*tauD.* ...
phiA).*(-1).*sigmaA+(-1).*fret.*sigmaDa+((-
1)+fret).*sigmaA.*(sigmaA+sigmaDa).*tauD.*phiA)+ ...
tauA.*((-1)+tauD.*phiA.*((-2)+fret).*(sigmaA+sigmaDa)+((-
1)+fret).*sigmaDa.*(2.*sigmaA+ ...
sigmaDa).*tauD.*phiA))).^(-1).*phiD.*(1+sigmaD.*tauD.*phiD).^(-1)];

solutions=vpasolve(subs(freteqs, ...
[i1 i2 i3 S1 S2 S3 S4 tauD tauA phiD phiA sigmaD sigmaDa sigmaA sigmaAd
alphaSat], ...
[i1num i2num i3num S1num S2num S3num S4num tauDnum tauAnum phiDnum phiAnum
sigmaDnum sigmaDanum sigmaAnum sigmaAdnum alphanum]),[fret Fd Fa]);

fretValues=double(solutions.fret(:));
FdValues=double(solutions.Fd(:));
FaValues=double(solutions.Fa(:));
IdValues=FdValues*Dsat0dnum;
IaValues=FaValues*Asat0anum;

```

```
solutionsTable=table(fretValues,IdValues,IaValues);
```

```

function
[solutions,solutionsTable]=fretWithSatFrustr_2(i1num,i2num,i3num,S1num,S2num,S3
num,S4num,tauDnum,tauAnum,sigmaDnum,sigmaDanum,sigmaAnum,sigmaAdnum,phiDnum,ph
iAnum)
% This function takes the saturation of donor and acceptor fluorescence and
% FRET frustration into consideration.
% Numerical solution for the Na=Nd case (only D-A complex, no free D or A).
%
% i1num,i2num,i3num - intensities measured in the donor, FRET and acceptor
channel, respectively
% S1num,S2num,S3num,S4num - overspill parameters
% tauDnum,tauAnum - fluorescence lifetime of the donor and acceptor,
respectively
% sigmaDnum,sigmaDanum - absorption cross-section of the donor at the donor
and acceptor excitation wavelength, respectively
% sigmaAnum,sigmaAdnum - absorption cross-section of the acceptor at the
acceptor and donor excitation wavelength, respectively
% phiDnum,phiAnum - photon flux of the donor- and acceptor-exciting laser,
respectively
%
% solutions - structure variable containing the solutions (FRET efficiency,
alpha, unquenched donor (Id) and directly-excited acceptor (Ia) intensity)
% solutionsTable - summary of the solutions in table format
%
% Peter Nagy, email: peter.v.nagy@gmail.com
Dsat0dnum=sigmaDnum.*tauDnum.*phiDnum.*(1+sigmaDnum.*tauDnum.*phiDnum).^(-1);
Dsat0anum=sigmaDanum.*tauDnum.*phiAnum.*(1+sigmaDanum.*tauDnum.*phiAnum).^(-
1);
Asat0dnum=sigmaAdnum.*tauAnum.*phiDnum.*(1+sigmaAdnum.*tauAnum.*phiDnum).^(-
1);
Asat0anum=sigmaAnum.*tauAnum.*phiAnum.*(1+sigmaAnum.*tauAnum.*phiAnum).^(-1);

syms i1 i2 i3 S1 S2 S3 S4 Fd Fa fret tauD tauA phiD phiA sigmaD sigmaDa sigmaA
sigmaAd Dsat0d Dsat0a Asat0d Asat0a
freteqs=[i1==Fd.*sigmaD.*tauD.*phiD.*(((-1)+fret).*tauD+tauA.^2.*phiD.*((-
1).*sigmaAd+(-1).* ...
    fret.*sigmaD+((-1)+fret).*sigmaAd.*(sigmaAd+sigmaD).*tauD.*phiD)+((-
1)+fret).*tauA.*(1+( ...
    2.*sigmaAd+sigmaD).*tauD.*phiD)).*(tauD.*((-1)+((-
1)+fret).*sigmaD.*tauD.*phiD)+tauA.^2.* ...
    phiD.*(1+sigmaD.*tauD.*phiD).*((-1).*sigmaAd+(-1).*fret.*sigmaD+((-
1)+fret).*sigmaAd.*( ...
    sigmaAd+sigmaD).*tauD.*phiD)+tauA.*((-1)+tauD.*phiD.*((-
2)+fret).*(sigmaAd+sigmaD)+((-1)+ ...
    fret).*sigmaD.*(2.*sigmaAd+sigmaD).*tauD.*phiD)).^(-1)+Asat0a.*Asat0d.^(-
1).*Fa.* ...
    S4.*tauA.*phiD.*((-
1)+fret).*sigmaAd.^2.*tauA.*tauD.*phiD.*(1+sigmaD.*tauD.*phiD)+(-1) ...
    .*fret.*sigmaD.*(tauA+tauD+sigmaD.*tauA.*tauD.*phiD)+sigmaAd.*((-1)+((-
1)+fret).*sigmaD.* ...
    tauD.*phiD).*(tauA+tauD+sigmaD.*tauA.*tauD.*phiD)).*(tauD.*((-1)+((-
1)+fret).*sigmaD.*tauD.* ...
    phiD)+tauA.^2.*phiD.*(1+sigmaD.*tauD.*phiD).*((-1).*sigmaAd+(-
1).*fret.*sigmaD+((-1)+ ...
    fret).*sigmaAd.*(sigmaAd+sigmaD).*tauD.*phiD)+tauA.*((-1)+tauD.*phiD.*((-
2)+fret).*( ...

```

```

sigmaAd+sigmaD)+((-1)+fret).*sigmaD.*(2.*sigmaAd+sigmaD).*tauD.*phiD)).^(-
1),...
i2==Fd.*S1.*sigmaD.*tauD.*phiD.*((-1)+fret).*tauD+tauA.^2.*phiD.*((-
1).*sigmaAd+(-1).* ...
fret).*sigmaD+((-1)+fret).*sigmaAd.*(sigmaAd+sigmaD).*tauD.*phiD)+((-
1)+fret).*tauA.*(1+( ...
2.*sigmaAd+sigmaD).*tauD.*phiD)).*(tauD.*((-1)+((-
1)+fret).*sigmaD.*tauD.*phiD)+tauA.^2.* ...
phiD.*(1+sigmaD.*tauD.*phiD).*((-1).*sigmaAd+(-1).*fret).*sigmaD+((-
1)+fret).*sigmaAd.*( ...
sigmaAd+sigmaD).*tauD.*phiD)+tauA.*((-1)+tauD.*phiD.*((-
2)+fret).* (sigmaAd+sigmaD)+((-1)+ ...
fret).*sigmaD.*(2.*sigmaAd+sigmaD).*tauD.*phiD)).^(-1)+Asat0a.*Asat0d.^(-
1).*Fa.* ...
S2.*tauA.*phiD.*((-
1)+fret).*sigmaAd.^2.*tauA.*tauD.*phiD.*(1+sigmaD.*tauD.*phiD)+(-1) ...
.*fret).*sigmaD.*(tauA+tauD+sigmaD.*tauA.*tauD.*phiD)+sigmaAd.*((-1)+((-
1)+fret).*sigmaD.* ...
tauD.*phiD).* (tauA+tauD+sigmaD.*tauA.*tauD.*phiD)).*(tauD.*((-1)+((-
1)+fret).*sigmaD.*tauD.* ...
phiD)+tauA.^2.*phiD.*(1+sigmaD.*tauD.*phiD).*((-1).*sigmaAd+(-
1).*fret).*sigmaD+((-1)+ ...
fret).*sigmaAd.*(sigmaAd+sigmaD).*tauD.*phiD)+tauA.*((-1)+tauD.*phiD.*((-
2)+fret).* ( ...
sigmaAd+sigmaD)+((-1)+fret).*sigmaD.*(2.*sigmaAd+sigmaD).*tauD.*phiD)).^(-
1),...
i3==Dsat0a.^(-1).*Dsat0d.*Fd.*S3.*sigmaDa.*tauD.*phiA.*((-1)+fret).*tauD+ ...
tauA.^2.*phiA.*((-1).*sigmaA+(-1).*fret).*sigmaDa+((-
1)+fret).*sigmaA.*(sigmaA+sigmaDa).* ...
tauD.*phiA)+((-
1)+fret).*tauA.*(1+(2.*sigmaA+sigmaDa).*tauD.*phiA)).*(tauD.*((-1)+((-
-1)+fret).*sigmaDa.*tauD.*phiA)+tauA.^2.*phiA.*(1+sigmaDa.*tauD.*phiA)).*( (-
1).*sigmaA+(-1) ...
.*fret).*sigmaDa+((-1)+fret).*sigmaA.*(sigmaA+sigmaDa).*tauD.*phiA)+tauA.*((-
1)+tauD.*phiA.*( ...
((-2)+fret).* (sigmaA+sigmaDa)+((-
1)+fret).*sigmaDa.*(2.*sigmaA+sigmaDa).*tauD.*phiA)).^( ...
-1)+Fa.*tauA.*phiA.*((-
1)+fret).*sigmaA.^2.*tauA.*tauD.*phiA.*(1+sigmaDa.*tauD.*phiA)+ ...
-1).*fret).*sigmaDa.*(tauA+tauD+sigmaDa.*tauA.*tauD.*phiA)+sigmaA.*((-1)+((-
1)+fret).* ...
sigmaDa.*tauD.*phiA).* (tauA+tauD+sigmaDa.*tauA.*tauD.*phiA)).*(tauD.*((-
1)+((-1)+fret).* ...
sigmaDa.*tauD.*phiA)+tauA.^2.*phiA.*(1+sigmaDa.*tauD.*phiA)).*( (-
1).*sigmaA+(-1).*fret.* ...
sigmaDa+((-1)+fret).*sigmaA.*(sigmaA+sigmaDa).*tauD.*phiA)+tauA.*((-
1)+tauD.*phiA.*((-2)+ ...
fret).* (sigmaA+sigmaDa)+((-
1)+fret).*sigmaDa.*(2.*sigmaA+sigmaDa).*tauD.*phiA)).^(-1)];

solutions=vpasolve(subs(freteqs,...
[i1 i2 i3 S1 S2 S3 S4 tauD tauA phiD phiA sigmaD sigmaDa sigmaA sigmaAd
Dsat0d Dsat0a Asat0d Asat0a],...
[i1num i2num i3num S1num S2num S3num S4num tauDnum tauAnum phiDnum phiAnum
sigmaDnum sigmaDanum sigmaAnum sigmaAdnum Dsat0dnum Dsat0anum Asat0dnum
Asat0anum]),[fret Fd Fa]);

```

```
fretValues=double(solutions.fret(:));
FdValues=double(solutions.Fd(:));
FaValues=double(solutions.Fa(:));
IdValues=FdValues*Dsat0dnum;
IaValues=FaValues*Asat0anum;
alphaValues=IaValues*S2num./IdValues*Dsat0dnum/Asat0dnum*tauAnum/tauDnum;
solutionsTable=table(fretValues,alphaValues,IdValues,IaValues);
```